NeuroImage 246 (2022) 118783

Contents lists available at ScienceDirect

NeuroImage

journal homepage: www.elsevier.com/locate/neuroimage

The neural coding of face and body orientation in occipitotemporal cortex

Celia Foster[a,b,c,*], Mintao Zhao[a,d], Timo Bolkart[b], Michael J. Black[b], Andreas Bartels[a,e,f,g], Isabelle Bülthoff[a,*]

[a] Max Planck Institute for Biological Cybernetics, Tübingen, Germany
[b] Max Planck Institute for Intelligent Systems, Tübingen, Germany
[c] International Max Planck Research School for Cognitive and Systems Neuroscience, University of Tübingen, Tübingen, Germany
[d] School of Psychology, University of East Anglia, United Kingdom
[e] Centre for Integrative Neuroscience, Tübingen, Germany
[f] Department of Psychology, University of Tübingen, Germany
[g] Bernstein Center for Computational Neuroscience, Tübingen, Germany

ARTICLE INFO

Keywords:
Orientation
Viewpoint
Body perception
Face perception
fMRI

ABSTRACT

Face and body orientation convey important information for us to understand other people's actions, intentions and social interactions. It has been shown that several occipitotemporal areas respond differently to faces or bodies of different orientations. However, whether face and body orientation are processed by partially overlapping or completely separate brain networks remains unclear, as the neural coding of face and body orientation is often investigated separately. Here, we recorded participants' brain activity using fMRI while they viewed faces and bodies shown from three different orientations, while attending to either orientation or identity information. Using multivoxel pattern analysis we investigated which brain regions process face and body orientation respectively, and which regions encode both face and body orientation in a stimulus-independent manner. We found that patterns of neural responses evoked by different stimulus orientations in the occipital face area, extrastriate body area, lateral occipital complex and right early visual cortex could generalise across faces and bodies, suggesting a stimulus-independent encoding of person orientation in occipitotemporal cortex. This finding was consistent across functionally defined regions of interest and a whole-brain searchlight approach. The fusiform face area responded to face but not body orientation, suggesting that orientation responses in this area are face-specific. Moreover, neural responses to orientation were remarkably consistent regardless of whether participants attended to the orientation of faces and bodies or not. Together, these results demonstrate that face and body orientation are processed in a partially overlapping brain network, with a stimulus-independent neural code for face and body orientation in occipitotemporal cortex.

1. Introduction

Human face and body orientation convey important cues about social interactions. The ability to process orientation information is therefore crucial for us to understand how other people interact with us and the world around them. For example, we use face and body orientation to infer that a person intends to interact with us when they face toward us, and does not when they turn their back to us. Person orientation is primarily determined by information from the face and body, though eye gaze (which indicates direction of attention) is often taken into consideration in social interaction scenarios (Nummenmaa and Calder, 2009). Psychological research has shown that these different sources of information are not processed independently in the perception of person orientation. For example, interactions have been found between face and body orientation information (Moors et al., 2015) and between face orientation and gaze direction information (Gibson and Pick, 1963; Wollaston, 1824). To what extent the neural processes underlying face and body orientation may interact with each other remains unclear.

Neuroimaging and electrophysiology studies have investigated which brain regions process information about face and body orientation in humans and macaque monkeys. For face orientation, human neuroimaging studies have found different patterns of response to different face orientations in the face-responsive occipital face area (OFA), fusiform face area (FFA) and posterior superior temporal sulcus (pSTS), as well as the object-responsive lateral occipital complex (LOC) and the

* Corresponding authors at: Celia Foster: Biopsychology and Cognitive Neuroscience, Faculty of Psychology and Sports Science, Bielefeld University, Germany; Isabelle Bülthoff: Max Planck Institute for Biological Cybernetics, Max-Planck-Ring 8, 72076 Tübingen, Germany.
E-mail addresses: celia.foster@uni-bielefeld.de (C. Foster), isabelle.buelthoff@tuebingen.mpg.de (I. Bülthoff).

https://doi.org/10.1016/j.neuroimage.2021.118783.
Received 14 August 2021; Received in revised form 9 November 2021; Accepted 4 December 2021
Available online 5 December 2021.

early visual cortex (Axelrod and Yovel, 2012; Guntupalli et al., 2017; Kietzmann et al., 2012; Natu et al., 2010; Ramírez et al., 2014). Similarly, for macaque monkeys, neurons in the middle lateral and middle fundus face-responsive patches and the anterior superior temporal sulcus (aSTS) have been shown to respond to specific face orientations (Dubois et al., 2015; Freiwald and Tsao, 2010; Perrett et al., 1985; Wachsmuth et al., 1994). For body orientation, human neuroimaging studies have shown that the body-responsive extrastriate body area (EBA) and fusiform body area (FBA) are sensitive to body orientation (Chan et al., 2004; Ewbank et al., 2011; Taylor et al., 2010; Vangeneugden et al., 2014). Furthermore, recent studies have shown that the EBA also responds higher to interacting people as compared to non-interacting people (Abassi and Papeo, 2020; Walbrin and Koldewyn, 2019). In macaques, body orientation can be decoded from both the middle and anterior STS body patches (Kumar et al., 2019). Body orientation responsive neurons have also been identified in the macaque aSTS (Wachsmuth et al., 1994).

While the above studies suggest that many occipitotemporal regions respond to face and/or body orientation, it remains unclear whether the observed neural responses reflect a high-level stimulus-independent encoding of orientation, or are driven by face- or body- specific features, such that the neural coding of a given face-orientation does not generalise to the neural coding of the corresponding body-orientation. Moreover, most previous studies have investigated the neural responses to the orientation of faces and bodies separately, leaving it an open question regarding whether face and body orientation are processed in completely separate or partially overlapping brain regions. There is some evidence that face- and body-responsive regions form independent and separated brain networks (Peelen and Downing, 2007; Premereur et al., 2016). However, other studies have shown that some categorical information (e.g. gender or weight) shared by faces and bodies can be coded in an abstract stimulus-independent manner (Foster et al., 2019; Ghuman et al., 2010). While human face and body orientation are often aligned with each other, few studies have tested whether this orientation alignment leads to a shared neural orientation code. Wachsmuth et al. (1994) found neurons in the macaque aSTS that responded to the orientation of faces and bodies displayed alone, despite remarkable differences in the low-level visual features between face and body images. This finding suggests that the neural coding of face and body orientation may be partially overlapping. As the study only recorded neural activity in the aSTS, whether other brain regions encode orientation in such a stimulus-independent manner remains unknown.

In this study, we investigated how face and body orientation information is processed in face- and body-responsive brain regions and, in particular, whether face and body orientation information is processed in completely separate or partially overlapping brain regions. To address this question, we recorded participants' brain activity using fMRI while they viewed images of faces and bodies from three different orientations. We trained linear support vector machine (SVM) classifiers to distinguish between patterns of neural activity evoked by the three stimulus orientations and then used them to predict stimulus orientation in a separate set of test data. To directly compare which brain regions respond to face and body orientation respectively, we performed multivoxel pattern analyses (MVPA) separately for neural activity evoked by faces and bodies. To investigate which brain regions encode orientation in a stimulus-independent manner that can generalize across faces and bodies, we trained classifiers on neural activity evoked by faces and tested them on neural activity evoked by bodies, and vice-versa. We performed these analyses in face- and body-responsive brain regions, as well as across the whole brain using searchlight analyses.

We also investigated whether the neural coding of face and body orientation was enhanced when participants attended to stimulus orientation in comparison to when they did not. Most studies that have investigated the neural coding of face orientation used tasks that directed attention away from orientation (e.g. detection of brightness change in Ramírez et al. (2014), or detection of identity repetition in Axelrod and Yovel (2012); Guntupalli et al. (2017)). These studies suggested that processing of face orientation information is relatively automatic (i.e. attending to stimulus orientation is not necessary). On the other hand, attending to face identity or facial expression has been shown to enhance the neural representation of these properties (Dobs et al., 2018; Foster et al., 2021; Guntupalli et al., 2017). For instance, Dobs et al. (2018) showed that decoding of face identities and facial expressions from neural responses were selectively improved for tasks involving explicit attention to identity and expression respectively. To test whether the neural coding of face and body orientation is modulated by task requirements, we had our participants perform two different behavioural tasks during fMRI scanning, one required attention to stimulus orientation, whereas the other required attention to stimulus identity. If the attention enhancement effect generalises to the processing of orientation, we would expect better decoding performance for the orientation task than the identity task.

2. Materials and methods

Data analyses presented here were conducted using a dataset that was collected as part of a larger study, with prior analyses focusing on face and body identity (Foster et al., 2021). Here we present novel findings investigating behavioural and neural responses to face and body orientation.

2.1. Participants

20 participants (14 female, 6 male, 21–51 years old) completed the experiment. All participants provided written informed consent prior to the experiment, and the experimental procedure was approved by the local ethics committee of the University Clinic Tübingen.

2.2. Stimuli

2.2.1. Main experiment stimuli

The experimental stimuli were images of faces and bodies shown from three different orientations, 0° (front), 45° (three-quarter view) and 90° (profile). Examples of the stimuli are shown in Fig. 1A. Face and body stimuli were created using face and body scans of three female individuals that were registered to a 3D facial shape and expression model for the face stimuli (Li et al., 2017) and a 3D body shape and pose model for the body stimuli (Loper et al., 2015). Body stimuli were shown in a standard A-pose (see Fig. 1A) and faces had a neutral expression. We brightened the texture obtained from the original scans and filled in any missing texture. Stimuli were shown in colour, and for body stimuli a grey rectangle was placed over the face, in order to exclude any face information from the body images. During the experiment face and body stimuli were shown at three different image sizes. Face stimuli had mean widths and heights of 4.4° x 6.4° (large), 3.6° x 5.2° (medium), and 2.8° x 4.0° (small) of visual angle, and body stimuli had mean widths and heights of 3.2° x 7.7° (large), 2.6° x 6.2° (medium), and 2.0° x 4.8° (small) of visual angle.

2.2.2. Localizer stimuli

Stimuli for the localizer experiment consisted of grayscale images of faces, headless bodies, objects and phase-scrambled images. Phase-scrambled images were Fourier-scrambled versions of a collage image containing the face and headless body images. None of the localizer stimuli were used as stimuli for the main experiment.

2.3. Experimental design

Participants lay supine in the MRI scanner and viewed the stimuli on a screen positioned 92 cm behind their head, which they viewed via a mirror attached to the head coil. The stimuli were presented using a projector (resolution 1920 × 1080), and the screen spanned 25°

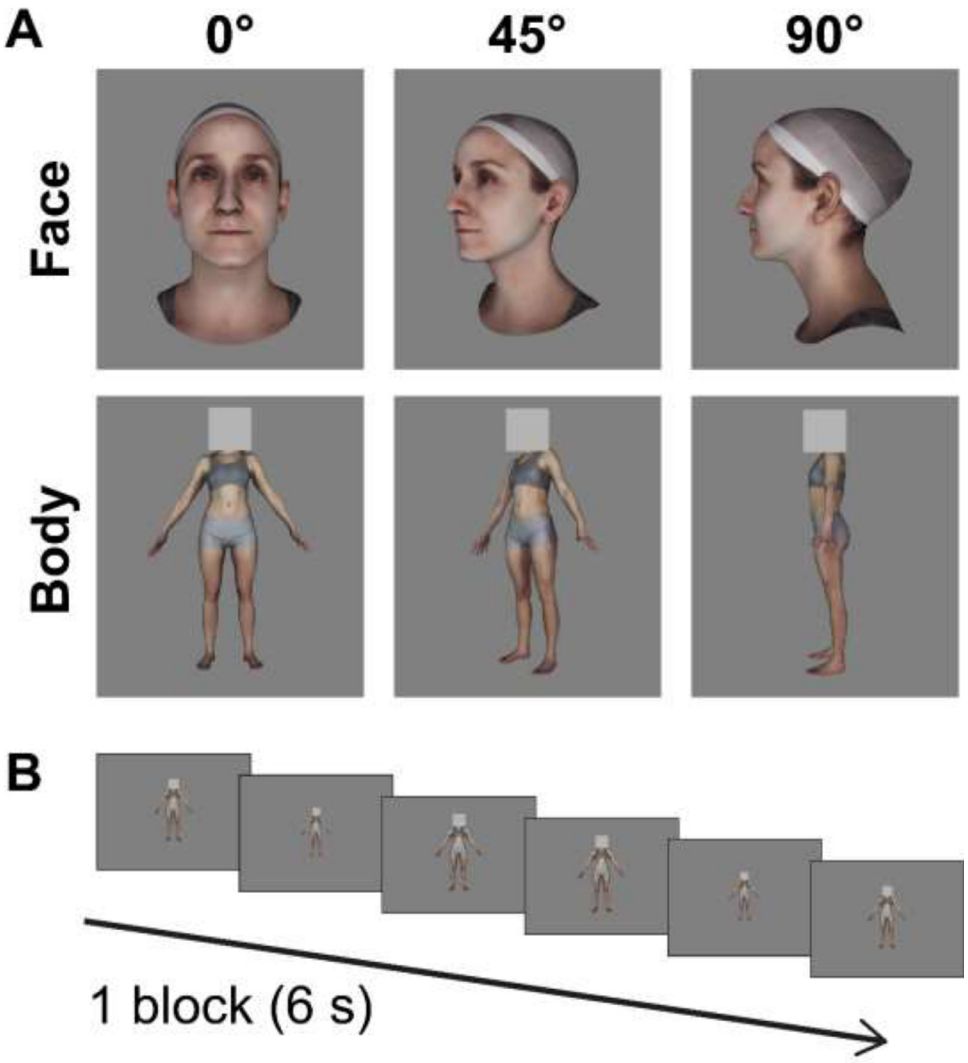

Fig. 1. Experimental stimuli and example stimulus block. (A) Face and body images were shown from three different orientations: 0° (front), 45° (three-quarter) and 90° (profile). (B) Stimuli were shown in a block design during the experiment, where stimuli within a block were all from one condition (i.e. face or body, one orientation, one identity) and varied in their image-size (three different image-sizes, each shown twice, presented in a random order). Each block was followed by 2 s fixation.

(horizontal) x 14° (vertical) of visual angle. The experiment was programmed with Matlab 2017a using the Psychophysics Toolbox extensions (Brainard, 1997; Kleiner et al., 2007) and run on Ubuntu 17.10.

2.3.1. Main experiment procedure

Each participant completed eight fMRI runs. Each run contained 18 different experimental conditions, resulting from a 2 (Stimuli type: face or body) x 3 (Orientation: 0°, 45°, or 90°) x 3 (Identity) factorial design. Stimuli were presented in a block design (Fig. 1B). Each block lasted 6 s followed by 2 s fixation before the next block began. This block length was used to increase fMRI signal by blocking the stimuli whilst ensuring runs did not become too long, and has been successfully used in previous fMRI MVPA paradigms (e.g. Bannert and Bartels, 2017, 2013; Foster et al., 2019). Each run contained 54 blocks (3 repetitions per condition). These 54 blocks per run were presented in groups of 18 blocks (all conditions presented in random order), each group preceded by and followed by 8 s of fixation. Thus, each condition was repeated at three time points spaced throughout the run. Each block contained 6 images that were all from the same condition (i.e. face or body, one orientation, one identity). Images within a block were shown at three different image-sizes with scale factors of 1, 1.3 and 1.6 (i.e. the largest image-size was 1.6 times both the width and height of the smallest image-size). Each block contained 2 repetitions of each image-size, shown in a random order. Each image in the block was shown for 0.9 s followed by a 0.1 s blank grey screen.

2.3.2. Main experiment task

We manipulated participants' attention to orientation and identity during the experiment. In half of the fMRI runs participants were instructed at the beginning of the run to respond at the end of each block to which orientation (i.e. 0°, 45° or 90°) was presented in the block. In the other half of the runs, participants were instructed to respond to which identity was presented in the block. Participants were trained to recognise the three identities prior to the fMRI experiment. Participants pressed a button with one of three fingers to indicate the orientation or identity shown in the block.

To maintain participants' attention to the stimuli throughout the block, we asked participants to perform an additional attention task in all runs. Participants were instructed to respond by pressing a button with their thumb immediately whenever they saw an image belonging to the smallest of our three image-sizes (scale factor 1, shown twice per block in a random order).

2.3.3. fMRI localizer experiment procedure

Participants completed one run of a localizer experiment following the main experiment. Data from this localizer experiment was used to define face- and body-responsive regions of interest (ROIs). The localizer experiment consisted of four stimulus conditions (faces, bodies, objects and phase-scrambled images) that were presented in a block design. Faces, bodies and objects were shown in front of the phase-scrambled images so that the size of the visual-field stimulation was the same for

Table 1
Average MNI coordinates and volume of each ROI (± standard deviations). N indicates the number of participants each ROI was identified in. ROI analyses were conducted in subject space and then ROIs were subsequently normalised to generate MNI coordinates.

ROI	hem	x			y			z			Volume (mm^3)			N
OFA	left	−35	±	6.7	−85	±	5.7	−11	±	3.5	770	±	379.9	20
	right	38	±	4.0	−81	±	5.8	−10	±	3.3	1009	±	378.6	20
FFA	left	−40	±	2.8	−55	±	6.1	−20	±	2.9	771	±	354.7	20
	right	43	±	3.3	−52	±	4.2	−18	±	2.4	1073	±	392.5	20
pSTS	left	−50	±	6.4	−62	±	8.8	17	±	10.2	519	±	541.2	19
	right	53	±	5.5	−54	±	10.0	12	±	8.9	732	±	403.1	20
ATFA	left	−34	±	5.4	−12	±	6.5	−33	±	6.6	172	±	117.4	15
	right	34	±	5.8	−8	±	5.5	−37	±	5.8	335	±	265.6	18
EBA	left	−44	±	3.7	−78	±	5.3	3	±	6.5	900	±	473.3	20
	right	49	±	2.3	−70	±	3.0	0	±	4.6	1632	±	503.2	20
FBA	left	−39	±	4.2	−50	±	6.3	−20	±	2.9	680	±	456.7	19
	right	41	±	4.1	−50	±	5.5	−18	±	3.0	1105	±	572.2	20
LOC	left	−41	±	3.9	−81	±	4.4	−2	±	5.2	696	±	284.0	20
	right	47	±	3.0	−74	±	3.9	−3	±	4.7	746	±	214.5	20
EVC	left	−12	±	1.8	−99	±	1.8	−2	±	3.1	1120	±	408.5	19
	right	19	±	2.1	−96	±	2.0	−1	±	2.9	1262	±	514.8	19

every image. Each block contained 8 images from one condition where each image was presented for 1.8 s followed by a 0.2 s blank grey screen. Different stimulus conditions were presented in a carryover counterbalanced sequence, so that each condition was preceded by each condition an equal number of times (Brooks, 2012).

During the localizer experiment, to ensure that participants kept their attention on the stimuli, they performed a one-back matching task on the images. Image repetitions occurred once every 9 s on average.

2.4. Imaging parameters

Images were acquired using a 3T Siemens Prisma scanner with a 64-channel head coil (Siemens, Erlangen, Germany). Functional T2* echo-planar images (EPI) were acquired using a sequence with the following parameters; multiband acceleration factor 2, GRAPPA acceleration factor 2, TR 1.84 s, TE 30 ms, flip angle 79°, FOV 192 × 192 mm. Volumes consisted of 60 slices, with an isotropic voxel size of 2 × 2 × 2 mm. The first 8 volumes of each run were discarded to allow for equilibration of the T1 signal. For each participant a high-resolution T1-weighted anatomical scan was acquired with the following parameters; TR 2 s, TE 3.06 ms, FOV 232 × 256 mm, 192 slices, isotropic voxel size of 1 × 1 × 1 mm.

2.5. MRI data preprocessing

MRI data was preprocessed with SPM12 (http://www.fil.ion.ucl.ac.uk/spm/). All functional images were slice-time corrected, realigned and coregistered to the anatomical image. ROI and whole-brain searchlight analyses were conducted on the unsmoothed data in subject space. The resulting searchlight maps were normalised to MNI (Montreal Neurological Institute) space, and spatially smoothed with a 6 mm Gaussian kernel to allow for comparisons across participants. For the whole-brain univariate analyses the data was normalized to MNI space and spatially smoothed with a 6 mm Gaussian kernel. Localizer data was kept in subject-space and spatially smoothed with a 6 mm Gaussian kernel.

2.6. Definition of regions of interest

We defined face- and body-responsive ROIs using fMRI data from our localizer experiment (Table 1). We defined four face-responsive ROIs the OFA, FFA pSTS and anterior temporal face area (ATFA) and two body-responsive ROIs, the EBA and FBA. For each participant, we initially attempted to define face-responsive ROIs using the contrast faces > objects and body-responsive ROIs using the contrast bodies > objects. If we could not define the ROIs using these contrasts then we attempted to define them using the contrasts faces > scrambled images and bodies > scrambled images. We first attempted to define ROIs using a threshold of $p < .001$ (uncorrected), and then reduced this threshold to $p < .01$ (uncorrected) if the ROI could not be reliably defined using the first threshold. This approach allowed us to localize smaller ROIs that were not possible to detect at higher thresholds, whilst avoiding that larger ROIs became overly enlarged. We selected ROIs by selecting all active voxels within a rectangle around the activated ROI cluster. Supplementary Tables S1 and S2 provide further details for each ROI about how many participants we used each contrast and threshold for. Table S3 shows the mean overlap of ROI voxels across participants. We were able to define all ROIs in at least one hemisphere for every participant, and we combined right and left hemisphere ROIs into a single bilateral ROI for each participant. OFA, FFA and EBA ROIs were bilateral in all participants. pSTS and FBA ROIs were bilateral in 19 out of 20 participants and unilateral in the right hemisphere for 1 participant for each ROI. ATFA ROIs were bilateral in 13 participants, unilateral in the right hemisphere for 5 participants and unilateral in the left hemisphere for 2 participants.

We defined three additional ROIs, the LOC and the left and right early visual cortex (EVC). We defined the LOC using fMRI data from our localizer experiment and the contrast objects > scrambled images, using a threshold of $p < .001$ (uncorrected). We combined left and right hemisphere ROIs to form one bilateral LOC ROI for each of our 20 participants. To define our EVC ROIs, we first defined an anatomical masque of the EVC that included V1 and V2 from the Julich-Brain atlas (Amunts et al., 2020). We then selected all EVC voxels that showed higher activation during all experimental conditions as compared to baseline, using a threshold of $p < .001$ (uncorrected). Thus, these left and right hemisphere EVC ROIs contained the portion of the EVC that was activated by our experimental stimuli.

As some of our ROIs overlapped, we additionally performed analyses with the face-responsive OFA and FFA excluding body-responsive overlapping voxels from the EBA and FBA respectively. Similarly, we performed additional analyses with the body-responsive EBA and FBA excluding face-responsive overlapping voxels from the OFA and FFA respectively. The LOC also overlaps to some extent with the OFA and EBA. Table S4 gives details of the extent of the overlap between ROIs before exclusion of voxels, and Table S5 gives details of overlap after exclusion of overlapping face- and body-responsive voxels.

We plotted the responses of our face-, body- and object-responsive ROIs to illustrate their category-selectivity to all conditions of the localizer (Fig. S1), and additionally plotted the responses of ROIs with overlapping voxels removed (Fig. S2). These figures show that all face-

responsive ROIs showed highest responses to faces, and the EBA showed highest responses to bodies. The FBA showed highest responses to faces including all FBA voxels, but showed highest responses to bodies when overlapping voxels from the FFA were removed. Surprisingly, the LOC showed higher responses to bodies than to objects, even when overlapping voxels from the EBA and OFA were removed (Fig. S2; $t_{18} = 4.47, p < .001$). This trend was present in 18 out of 19 LOC ROIs with overlapping voxels removed. The LOC is traditionally defined by its higher responses to objects as compared to scrambled images (Malach et al., 1995), however this finding suggests that it shows even stronger responses to bodies than to general objects.

2.7. Behavioural analyses

Participants were instructed to respond with a button press at the end of each block to indicate which orientation or identity was presented in the block (one half of blocks orientation task, the other half of blocks identity task). We measured participants' behavioural performance using accuracy (% correct). To investigate whether detection of orientation or identity was different between the three stimuli orientations, we performed one-way repeated-measures ANOVAs with three levels (0°, 45° and 90° stimulus orientation). We corrected for non-sphericity where necessary following a Mauchly's test of sphericity. Following any significant ANOVA results, we performed follow-up paired *t*-tests between all combinations of the three orientation conditions to determine exactly which conditions showed differences in behavioural performance.

2.8. Univariate analyses

We conducted univariate analyses to investigate if there were brain regions that showed different mean levels of neural responses to faces or bodies of different orientations and whether behavioural task modulated these neural responses. Following preprocessing, we modelled the fMRI data with a GLM using SPM12, where the neural responses to each condition were modelled as separate regressors. We performed univariate analyses in ROIs and in whole-brain analyses.

For ROIs, we first performed 3 (Orientation) x 9 (ROI) x 2 (Behavioural Task) repeated-measures ANOVAs to investigate whether there were differences in the neural responses to different face/body orientations and whether the orientation responses differed across ROIs or behavioural task. We then conducted one-way repeated measures ANOVAs in each ROI to test which ROIs showed different responses to the three face and body orientations (i.e. 0°, 45° and 90°). We assessed significance using a threshold of $p < .05$, corrected for non-sphericity where necessary following a Mauchly's test of sphericity. In ROIs showing significant differences in the ANOVA analyses, we performed follow up paired *t*-tests to determine which stimulus orientations showed differences in neural activation.

For whole-brain analyses, we performed 3 (Orientation) x 2 (Behavioural Task) ANOVAs separately for face and body orientations to test which regions showed differences in responses to different orientations and whether these responses were modulated by behavioural task. We assessed significance with a threshold of $p < .05$, FWE corrected.

2.9. Multivoxel pattern analyses (MVPA)

We conducted multivoxel pattern analyses (MVPA) to investigate which brain regions contain different patterns of activity to faces and bodies of different orientations (0°, 45° and 90°). Following preprocessing, fMRI data was modelled with a General Linear Model (GLM) using SPM12, where the neural responses to each block were modelled as separate regressors in the GLM. MVPA analyses were then performed on the beta weight images with The Decoding Toolbox (Hebart et al., 2015) using a linear support vector machine classifier (LIBSVM) and a one-vs.-one winner-takes-all multiclass classification approach. We performed feature-scaling on the input data using z-score normalization and set any outlier values (values that were greater than 2 standard deviations from the mean) to 2 or −2. We estimated the mean and standard deviation for feature-scaling using the training data and then applied these values to the test data.

In the first set of MVPA analyses, we aimed to determine which brain regions contain separable patterns of activity to faces of different orientations and to bodies of different orientations. Thus, we analysed fMRI data evoked by face and body stimuli separately. We analysed fMRI data from the two behavioural tasks separately, thus we used 4 runs of fMRI data per analysis. In each analysis, we trained a linear SVM classifier to distinguish between neural activity evoked by the three stimulus orientations. We trained the classifier using neural activity data evoked by 2 of the 3 stimulus identities and from 3 of the 4 runs of fMRI data. We then tested the classifier on its ability to predict the three stimulus orientations from neural activity data evoked by the third stimulus identity from the 4th left-out run of fMRI data. Thus, if a brain region shows higher-than-chance decoding performance it must contain separable patterns of neural activity evoked by the three different stimulus orientations that can generalize across the stimulus identity. We used a 4-fold cross-validation procedure where we repeated the analysis 4 times with each run used once as the held out test dataset. We also repeated the analysis 3 times with each stimulus identity used as the held out test identity once. The final decoding accuracy was determined by averaging over the 4 cross-validation and 3 stimulus identity combinations.

In the second set of MVPA analyses, we aimed to determine which brain regions contain separable patterns of neural activity to the three stimulus orientations that could generalize across face and body stimuli. A region showing successful decoding in this analysis would suggest it encodes orientation, regardless of the stimuli being faces or bodies. We again analysed fMRI data from the two behavioural tasks separately and used 4 runs of data per analysis. We trained a linear SVM classifier to distinguish between neural activity evoked by the three stimulus orientations, using neural activity data evoked by face stimuli from 3 of the 4 runs of fMRI data. We then tested the classifier on its ability to predict the three stimulus orientations from neural activity data evoked by body stimuli from the 4th left out run of fMRI data. We again used a 4-fold cross-validation procedure where we repeated the analysis 4 times with each run used once as the held out test dataset. In addition, we repeated the analysis but using neural activity data evoked by body stimuli as the training set and neural activity data evoked by face stimuli as the test dataset. The final decoding accuracy was determined by averaging over the 4 cross-validation and the two training and test dataset combinations.

We conducted all MVPA analyses in ROIs and whole-brain searchlight analyses. For ROI analyses, we first performed 9 (ROI) x 2 (Behavioural Task) repeated-measures ANOVAs to test whether there were differences in orientation classification across ROIs or behavioural task. We then used permutation testing to determine which ROIs showed higher than chance classification performance. For each ROI we repeated each analysis 10,000 times with the condition labels assigned in a random order, in order to generate a null distribution of classification accuracies that would be expected by chance. We assessed significance by testing whether the actual mean decoding performance was higher than the 95th percentile of the null distribution, i.e. a significance threshold of $p < .05$ (see Schreiber and Krekelberg, 2013 for an overview of permutation testing methods in MVPA). We additionally used a Bonferroni correction to adjust for multiple comparisons ($N = 9$ ROIs tested). Next, we performed paired *t*-tests between ROIs that did and did not show higher-than-chance decoding performance, in order to test if there were significant differences in decoding performance between these pairs of ROIs. Corrections for multiple comparisons were not performed for follow-up tests. Lastly, we tested whether there were differences between face and body orientation classification across ROIs or behavioural task, with a 2 (Classification of Face or Body orientation) x 9 (ROI) x 2 (Behavioural Task) repeated measures ANOVA.

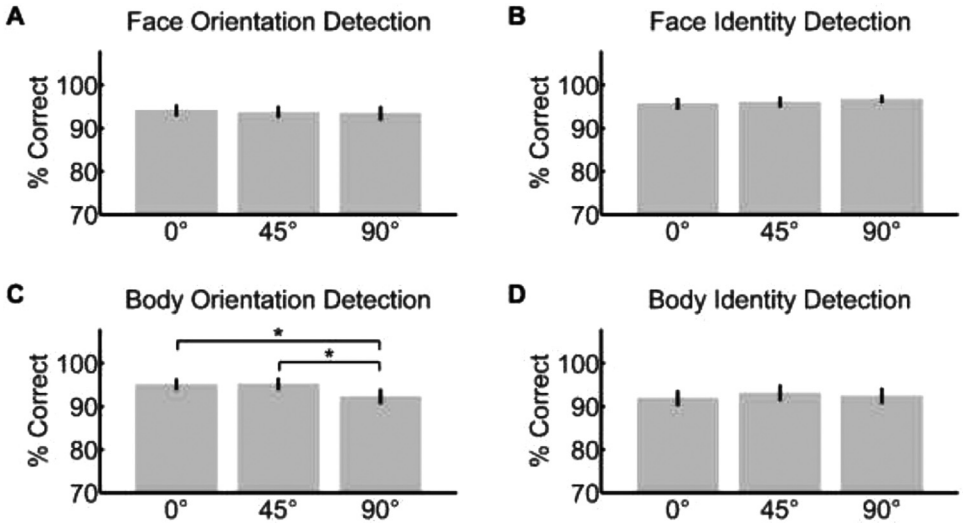

Fig. 2. Accuracy (% correct) in detection of orientation and identity for stimuli from the three different orientation conditions. (A) and (C) show participants accuracy in detecting the orientation of face (A) and body (C) stimuli. (B) and (D) show participants accuracy in detecting the identity of face (B) and body (D) stimuli. Error bars indicate ±1 SEM. * indicates $p <$ .05, paired *t*-test.

We performed whole-brain searchlight analyses in subject-space using 4-voxel radius spheres, which were centred around each voxel in the brain once. Thus for each participant and each analysis we obtained a whole-brain map of classification accuracies. These maps were then normalised to MNI space and smoothed with a 6 mm Gaussian kernel to allow for comparisons across participants. First, we performed paired *t*-test between searchlight results from the two behavioural tasks to test whether there were differences in decoding performance across the two tasks, using a threshold of $p < .05$, family-wise error rate (FWE) to correct for multiple comparisons. If no significant differences were identified, we combined searchlight results from the two behavioural tasks. Next, to test which regions showed higher than chance orientation decoding performance, we used SnPM13 (http://warwick.ac.uk/snpm) to assess significance using nonparametric permutation tests (Nichols and Holmes, 2001) with 10,000 permutations and 6 mm FWHM variance smoothing. This method uses a nonparametric sign-flip method to generate a group null distribution (Nichols and Holmes, 2001), and we tested for significance using a one-sided *t*-test with a threshold of $p <$ .05, family-wise error rate (FWE) corrected for multiple comparisons. Lastly, we performed a 2 (Classification of Face or Body orientation) x 2 (Task) whole-brain ANOVA to test if there were differences between face and body orientation classification, or any interaction between face and body orientation classification and behavioural task, and used a threshold of $p < .05$, family-wise error rate (FWE) to correct for multiple comparisons.

2.10. Data and code availability statement

Data cannot be shared as participants were informed that their data would be stored confidentially, in accordance with the rules of the local ethics committee. Code is available at: https://osf.io/uwb48/

3. Results

3.1. Behavioural results

Participants' mean accuracy in detecting the orientation and identity of stimuli of the three different stimulus orientations (0°, 45° and 90°) during the fMRI experiment is shown in Fig. 2.

3.1.1. Orientation detection

For the orientation detection task, participants showed a high accuracy for both face and body stimuli across all conditions (face stimuli: 93.8%; body stimuli: 94.3%). A one-way repeated-measures ANOVA showed there were no differences in face orientation detection performance between different orientations ($F_{2,38} = 0.23$, $p = .79$, $\eta_p^2 = 0.012$; Fig. 2A). In contrast, body orientation detection performance was different between the three orientations ($F_{2,38} = 3.54$, $p = .039$, $\eta_p^2 = 0.16$; Fig. 2C). Follow-up paired *t*-tests showed that detection accuracy was lower for 90° body stimuli than for 45° ($M = -2.9\%$, $SE = 1.31$, $t_{19} = -2.2$, $p = .039$, Cohen's $d_z = 0.50$) and 0° body stimuli ($M = -2.8\%$, $SE = 1.21$, $t_{19} = -2.3$, $p = .033$, Cohen's $d_z = 0.54$). There was no difference in detection accuracy between 45° and 0° body stimuli ($M = 0.1\%$, $SE = 1.18$, $t_{19} = 0.12$, $p = .91$, Cohen's $d_z = 0.026$). Note that overall detection accuracy was very high for all three body orientations (0°: 95.1%, 45°: 95.3%, 90°: 92.4%), showing that participants could easily detect all three body orientations.

3.1.2. Identity detection

For the identity detection task, participants showed high accuracy for both face (96.2%, Fig. 2B) and body (92.5%, Fig. 2D) stimuli. One-way repeated-measures ANOVAs showed no differences in identity detection across the three orientations (face stimuli, $F_{2,38} = 0.68$, $p = .51$, $\eta_p^2 = 0.035$; body stimuli, $F_{2,38} = 0.30$, $p = .74$, $\eta_p^2 = 0.016$). This result shows that participants could detect the stimulus identities equally well regardless of the orientation of the stimuli.

3.2. Univariate fMRI analyses

3.2.1. Face orientation responses

To investigate whether faces of different orientations evoked different mean levels of neural activity, we first conducted a 3 (Orientation) x 9 (ROI) x 2 (Task) repeated-measures ANOVA to investigate if there were differences in the neural responses to different face orientations, and whether any differences varied across ROIs or the behavioural task performed. We found a significant main effect of Orientation ($F_{2,36} = 15.80$, $p < .001$, $\eta_p^2 = 0.47$), as well as a significant interaction between Orientation and ROI ($F_{16,288} = 29.17$, $p < .001$, $\eta_p^2 = 0.62$), but no interaction between Orientation and Task ($F_{2,36} = 0.66$, $p = .52$, $\eta_p^2 = 0.04$) or triple-interaction between Orientation, ROI and Task ($F_{16,288} = 1.09$, $p = .36$, $\eta_p^2 = 0.06$). As we did not find any interaction with participant's behavioural task, we combined results from the two tasks for further analyses exploring the univariate face orientation responses in our ROIs.

To test which ROIs showed different overall levels of neural activity to faces of different orientations, we conducted one-way repeated measures ANOVAs with 3 levels (0°, 45° and 90°). Results are shown in Fig. 3 and results are shown for each participant in Fig. S3 and S4.

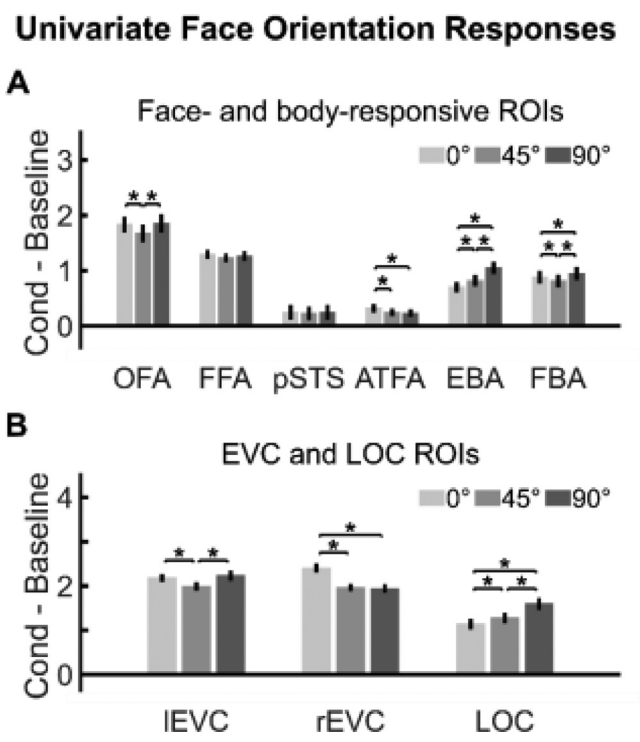

Fig. 3. Differences in mean BOLD responses (beta estimates) to faces of different orientations in face- and body-responsive ROIs (A) and EVC and LOC ROIs (B). * indicates $p < .05$, paired *t*-test. Error bars indicate ±1 SEM.

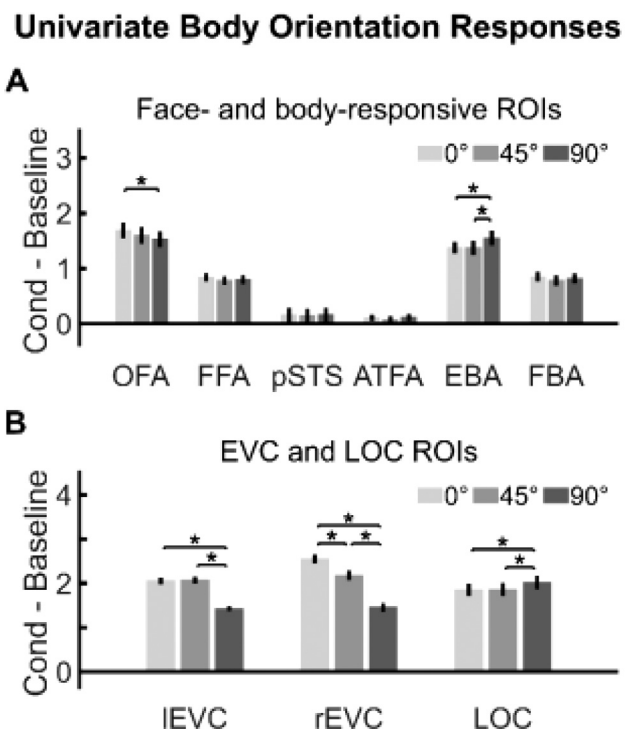

Fig. 4. Differences in mean BOLD responses (beta estimates) to bodies of different orientations in face- and body-responsive ROIs (A) and EVC and LOC ROIs (B). * indicates $p < .05$, paired *t*-test. Error bars indicate ±1 SEM.

For face-responsive ROIs, we found a significant effect of face orientation in the face-responsive OFA ($F_{2,38} = 8.00$, $p = .001$, $\eta_p^2 = 0.30$) and ATFA ($F_{2,38} = 4.36$, $p = .020$, $\eta_p^2 = 0.19$), but not in the FFA ($F_{2,38} = 2.62$, $p = .09$, $\eta_p^2 = 0.12$) or pSTS ($F_{2,38} = 0.29$, $p = .75$, $\eta_p^2 = 0.01$). There was also a significant effect of face orientation condition in the body-responsive EBA ($F_{2,38} = 99.32$, $p < .001$, $\eta_p^2 = 0.84$) and FBA ($F_{2,38} = 11.92$, $p < .001$, $\eta_p^2 = 0.39$), as well as the left and right EVC (lEVC: $F_{2,36} = 7.57$, $p = .010$ Greenhouse-Geisser corrected for non-sphericity, $\eta_p^2 = 0.30$; rEVC: $F_{2,36} = 46.13$, $p < .001$, $\eta_p^2 = 0.72$) and object-responsive LOC ($F_{2,38} = 64.61$, $p < .001$, $\eta_p^2 = 0.77$). Table S6 shows the results of follow-up paired *t*-tests investigating which orientations showed significant differences in ROIs that showed differences in face orientation responses. We additionally performed a 3 (Orientation) x 2 (Task) whole-brain ANOVA to investigate if any other brain regions showed a significant effect of orientation or interaction between orientation and behavioural task, but did not identify any significant regions in this analysis.

3.2.2. Body orientation responses

To test whether different body orientations evoked different mean levels of neural activity, we conducted a 3 (Orientation) x 9 (ROI) x 2 (Task) repeated-measures ANOVA. This allowed us to investigate whether there were differences in the neural responses to bodies of different orientations, and whether responses varied across ROIs or across the two behavioural tasks. We found a significant main effect of Orientation ($F_{2,36} = 22.59$, $p < .001$, $\eta_p^2 = 0.56$) and a significant interaction between Orientation and ROI ($F_{16,288} = 86.87$, $p < .001$, $\eta_p^2 = 0.83$), but no interaction between Orientation and Task ($F_{2,36} = 1.47$, $p = .24$, $\eta_p^2 = 0.08$) or triple-interaction between Orientation, ROI and Task ($F_{16,288} = 0.85$, $p = .62$, $\eta_p^2 = 0.05$). As we did not find an interaction with the behavioural task, we combined results from the two tasks for further analyses exploring univariate body orientation responses in our ROIs.

To investigate which ROIs showed different overall levels of neural activity to bodies of different orientations, we conducted one-way repeated measures ANOVAs with 3 levels (0°, 45° and 90°). The results are shown in Fig. 4 and results are shown for each participant in Fig. S5 and S6. For the face and body-responsive ROIs, we found significant differences in BOLD response to body orientation in the body-responsive EBA ($F_{2,38} = 12.61$, $p < .001$, $\eta_p^2 = 0.40$) and face-responsive OFA ($F_{2,38} = 6.42$, $p = .004$, $\eta_p^2 = 0.25$), but not in any other body- or face-responsive ROIs (FBA: $F_{2,38} = 2.01$, $p = .15$, $\eta_p^2 = 0.10$; FFA: $F_{2,38} = 2.20$, $p = .12$, $\eta_p^2 = 0.10$; pSTS: $F_{2,38} = 0.13$, $p = .88$, $\eta_p^2 = 0.01$; ATFA: $F_{2,38} = 1.00$, $p = .38$, $\eta_p^2 = 0.05$). We also found significant differences in responses to different body orientations in the left and right EVC (lEVC: $F_{2,36} = 2.57$, $p < .001$ Greenhouse-Geisser corrected for non-sphericity, $\eta_p^2 = 0.80$; rEVC: $F_{2,36} = 143.40$, $p < .001$, $\eta_p^2 = 0.89$) and object-responsive LOC ($F_{2,38} = 17.33$, $p < .001$, $\eta_p^2 = 0.48$). Results of follow-up paired *t*-tests to investigate which body orientations showed response differences in the OFA, EBA, left and right EVC and LOC, are shown in Table S7. We also conducted a 3 (Orientation) x 2 (Task) whole-brain ANOVA to investigate if any other brain regions showed differences in body orientation responses or an interaction between body orientation and behavioural task, but we did not identify any significant regions in this analysis.

3.3. Classification of face orientation

We first investigated which brain regions show face orientation-specific patterns of neural activity that could generalize across face identity. We trained a linear SVM classifier to distinguish between patterns of neural activity evoked by the three face orientations of two identities. We then tested the classifier on its ability to decode the face orientation of the third identity, using neural activity data in a left out run of data. We used a leave one run out cross validation method, and also repeated the analysis with each identity used once as the test identity. We performed the analysis in face- and body-responsive ROIs as well as in searchlight analyses across the whole brain. The results are shown in Fig. 5 and classifier confusion matrices are shown in Fig. S7.

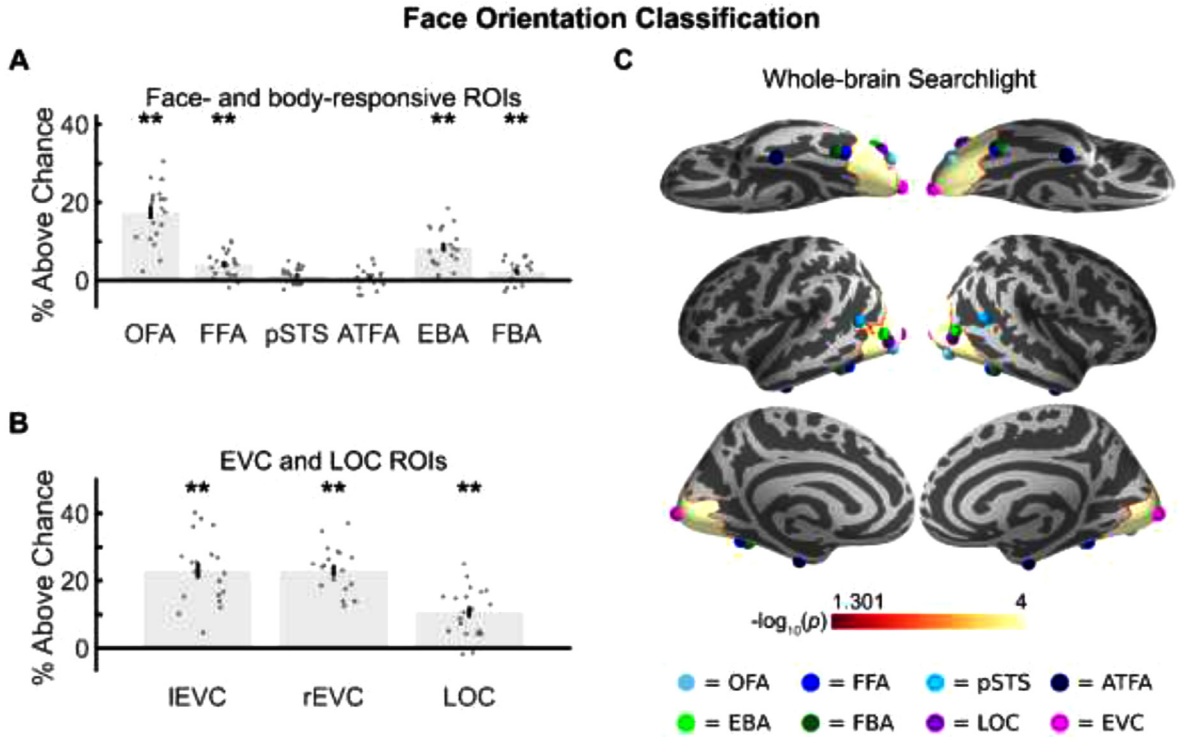

Fig. 5. Classification of face orientation. Classification accuracies for face- and body responsive ROIs (A) and EVC and LOC ROIs (B) are shown as their % above chance-level (1/3). Grey scatter points show classification accuracies for individual participants, ** indicates $p < .001$, * indicates $p < .05$, permutation test and Bonferroni corrected for $N = 9$ ROIs. (C) shows classification of face orientation in a whole-brain searchlight analysis. The scale bar shows $-\log_{10}(p$ values) between 1.301 ($p = .05$) and 4 ($p = 1 \times 10^{-4}$), FWE corrected.

3.3.1. ROI analyses

We first conducted a 9 (ROI) x 2 (Task) repeated-measures ANOVA to test whether face orientation classification differed across ROIs or was influenced by the behavioural task performed by the participants. We found a significant main effect of ROI ($F_{8,144} = 69.92$, $p < .001$, $\eta_p^2 = 0.80$), but no main effect of Task ($F_{1,18} = 0.03$, $p = .869$, $\eta_p^2 = 0.00$) or interaction between the two factors ($F_{8,144} = 1.69$, $p = .106$, $\eta_p^2 = 0.09$). Thus, decoding performance differed across our ROIs, but was unaffected by behavioural task. Therefore, we pooled results from the two behavioural tasks for further face orientation classification analyses.

To test from which ROIs we could decode face orientation at higher than chance-level (1/3), we conducted permutation tests in each ROI, Bonferroni-corrected for $N = 9$ ROIs. Classification of face orientation was significantly above chance-level (1/3) in the face-responsive OFA (50.8%, $p < .001$ Bonferroni-corrected, Cohen's $d_z = 2.35$) and FFA (37.5%, $p < .001$ Bonferroni-corrected, Cohen's $d_z = 1.26$), but not in the pSTS (34.7%, $p = .019$ uncorrected, Cohen's $d_z = 0.65$) or the ATFA (33.8%, $p = .21$ uncorrected, Cohen's $d_z = 0.21$). Interestingly, both body-responsive ROIs also showed above chance classification of face orientation (EBA: 41.9%, $p < .001$ Bonferroni-corrected, Cohen's $d_z = 1.71$; FBA: 35.7%, $p < .001$ Bonferroni-corrected, Cohen's $d_z = 0.81$). Classification of face orientation was also significantly above chance in the left and right EVC (lEVC: 56.4%, $p < .001$ Bonferroni-corrected, Cohen's $d_z = 2.28$; rEVC: 56.4%, $p < .001$ Bonferroni-corrected, Cohen's $d_z = 3.25$) and the object-responsive LOC (44.1%, $p < .001$ Bonferroni-corrected, Cohen's $d_z = 1.46$).

As face- and body-responsive ROIs can partially overlap (Schwarzlose et al., 2005), we conducted a follow-up test to investigate whether decoding performance was still significantly above chance level if body-responsive voxels were excluded from OFA and FFA ROIs, and if face-responsive voxels were excluded from EBA and FBA ROIs (Fig. 6). We found we could still decode face orientation

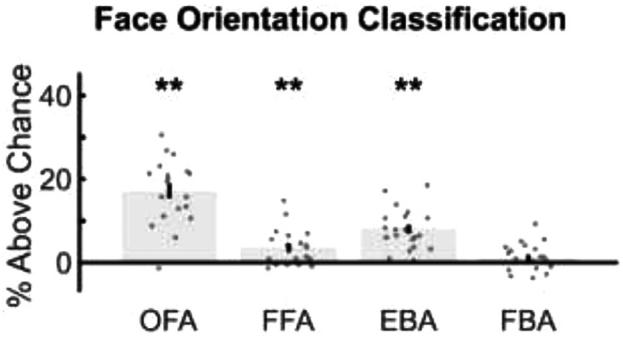

Fig. 6. Classification of face orientation in face- and body-responsive ROIs, with overlapping face- and body-responsive voxels excluded. Classification accuracies are shown as their % above chance-level (1/3). Grey scatter points show classification accuracies for individual participants, ** indicates $p < .001$, * indicates $p < .05$, permutation test and Bonferroni corrected for $N = 9$ ROIs.

significantly above chance level from the OFA, FFA and EBA (OFA: 50.5%, $p < .001$ Bonferroni-corrected, Cohen's $d_z = 2.23$; FFA: 37.0%, $p < .001$ Bonferroni-corrected, Cohen's $d_z = 0.85$; EBA: 41.3%, $p < .001$ Bonferroni-corrected, Cohen's $d_z = 1.62$), but not from the FBA (34.3%, $p = .057$ uncorrected, Cohen's $d_z = 0.26$). Thus, it seems that face orientation decoding in the FBA was driven by overlapping voxels from the neighbouring FFA.

To test whether face orientation classification performance was significantly higher in the face- and body-responsive ROIs where we found higher than chance classification performance (i.e. the OFA, FFA and EBA) as compared to face- and body-responsive ROIs that did not show higher than chance face orientation classification (i.e. pSTS, ATFA and FBA excluding face-responsive voxels) we conducted paired *t*-tests be-

Table 2
Results of paired *t*-tests comparing differences in face orientation classification performance between face- and body-responsive ROIs. In these tests the FFA ROI included overlapping body-responsive voxels, but face-responsive voxels were excluded from the FBA ROI.

Paired *t*-test	Mean difference	Standard error	*t* value	*p* value	Cohen's d_z
OFA vs. pSTS	16.96%	1.260	13.46	< 0.001	2.29
OFA vs. ATFA	17.79%	1.566	11.36	< 0.001	3.09
OFA vs. FBA	17.42%	1.825	9.55	< 0.001	2.19
FFA vs. pSTS	3.02%	0.801	3.77	.001	0.87
FFA vs. ATFA	3.85%	0.951	4.05	< 0.001	0.93
FFA vs. FBA	3.48%	1.130	3.08	.006	0.71
EBA vs. pSTS	7.50%	0.804	9.34	< 0.001	2.14
EBA vs. ATFA	8.33%	1.221	6.82	< 0.001	1.57
EBA vs. FBA	7.97%	1.391	5.73	< 0.001	1.31

tween each pair of ROIs. These tests confirmed that face orientation classification was significantly higher in the OFA, FFA and EBA than in the pSTS, ATFA and FBA ROI excluding face-responsive voxels. Full results of these paired *t*-tests are shown in Table 2.

3.3.2. Searchlight analyses

We conducted whole-brain searchlight analyses to investigate if any additional brain regions showed different patterns of responses to different face orientations. First, we conducted a paired *t*-test between searchlight face orientation decoding results from the orientation and identity recognition tasks, to test whether any regions showed differences in face orientation responses depending on the behavioural task performed. We found a significantly higher activity in the left motor cortex during the orientation recognition task compared to the identity recognition task. This is due to participants' responding using button presses with different fingers to indicate which orientation was shown in the block during the orientation recognition task. As no other regions showed any significant differences in responses between the two recognition tasks, we combined results from the two behavioural tasks for further face orientation searchlight analyses.

Our searchlight analysis showed that face orientation could be decoded from a large area of occipitotemporal cortex (Fig 5C). Consistent with our ROI results, this region included both the face-responsive OFA, the body-responsive EBA and object-responsive LOC, as well as the early visual cortex, and spread to the posterior fusiform gyrus adjacent to the FFA.

3.4. Classification of body orientation

We performed the same classification analyses to investigate the neural responses to body orientation as we used to investigate the neural responses to face orientation in Section 3.3. The results are shown in Fig. 7 and classifier confusion matrices are shown in Fig. S8.

3.4.1. ROI analyses

To test whether body orientation classification differed across ROIs or behavioural task, we conducted a 9 (ROI) x 2 (Task) repeated-measures ANOVA. This revealed a significant main effect of ROI ($F_{8,144}$ = 77.14, p < .001, η_p^2 = 0.81), but no main effect of Task ($F_{1,18}$ = 0.11, p = .747, η_p^2 = 0.01) or interaction between the two factors ($F_{8,144}$ = 1.20, p = .302, η_p^2 = 0.06). Thus, decoding performance differed across our ROIs, but was unaffected by behavioural task. Therefore, as previously, we pooled results from the two behavioural tasks for further body orientation classification analyses.

To test in which ROIs we could decode body orientation at a higher-than-chance level (1/3), we conducted permutation tests in each ROI, Bonferroni-corrected for N = 9 ROIs. Classification of body orientation was significantly above chance-level (1/3) in the body-responsive EBA (40.8%, p < .001 Bonferroni corrected, Cohen's d_z = 2.61) and the face-responsive OFA (42.9%, p < .001 Bonferroni corrected, Cohen's d_z = 1.35). Classification of body orientation was not significantly higher than chance in the body-responsive FBA (34.5%, p = .027 uncorrected, Cohen's d_z = 0.54) or face-responsive FFA (34.6%, p = .019 uncorrected, Cohen's d_z = 0.54), pSTS (32.4%, p = .92 uncorrected, Cohen's d_z = 0.36) or ATFA (33.8%, p = .232 uncorrected, Cohen's d_z = 0.20). For early visual and object-responsive ROIs, classification of body orientation was significantly above chance for both left and right EVC (lEVC: 52.9%, p < .001 Bonferroni corrected, Cohen's d_z = 2.67; rEVC: 59.8%, p < .001 Bonferroni corrected, Cohen's d_z = 2.64) and the LOC (40.5%, p < .001 Bonferroni corrected, Cohen's d_z = 1.62).

To test whether any overlapping voxels between the face-responsive OFA and body-responsive EBA might have contributed to body orientation classification in these ROIs, we conducted a follow-up test to investigate if decoding performance was still above chance-level if body-responsive voxels were excluded from OFA ROI, and face-responsive voxels were excluded from the EBA ROI. We found that body orientation decoding was still significantly above chance-level in both ROIs (EBA: 40.1%, p < .001 Bonferroni corrected, Cohen's d_z = 2.24; OFA: 43.4%, p < .001 Bonferroni corrected, Cohen's d_z = 1.40).

To investigate whether body orientation classification performance was significantly higher in the body-responsive EBA and face-responsive OFA, where we found higher than chance classification performance, as compared to face- and body-responsive ROIs that did not show higher than chance body orientation classification, we conducted paired *t*-tests between these ROIs. These tests confirmed that body orientation classification was significantly higher in the EBA and OFA compared to the FBA, FFA, pSTS, and ATFA. Full results of these paired *t*-tests are shown in Table 3.

3.4.2. Searchlight analyses

We conducted whole-brain searchlight analyses to investigate if any additional brain regions showed different patterns of responses to different body orientations. First, we conducted a paired *t*-test between results from the orientation and identity recognition tasks, to test whether any regions showed differences in body orientation responses depending on the behavioural task performed. We did not find any significant regions in this analysis, therefore we combined results from the two behavioural tasks for further body orientation searchlight analyses. We found that we could decode body orientation from a large area of occipitotemporal cortex, including the early visual cortex (Fig 7C). This region also overlapped with the mean coordinates of the EBA, OFA and LOC.

3.5. Comparison between face and body orientation classification

We performed further analyses to investigate whether there were differences in the regions encoding face and body orientation information.

3.5.1. ROI analyses

First, we performed a 2 (Face/Body orientation responses) x 9 (ROI) x 2 (Task) repeated measures ANOVA to test whether there were signif-

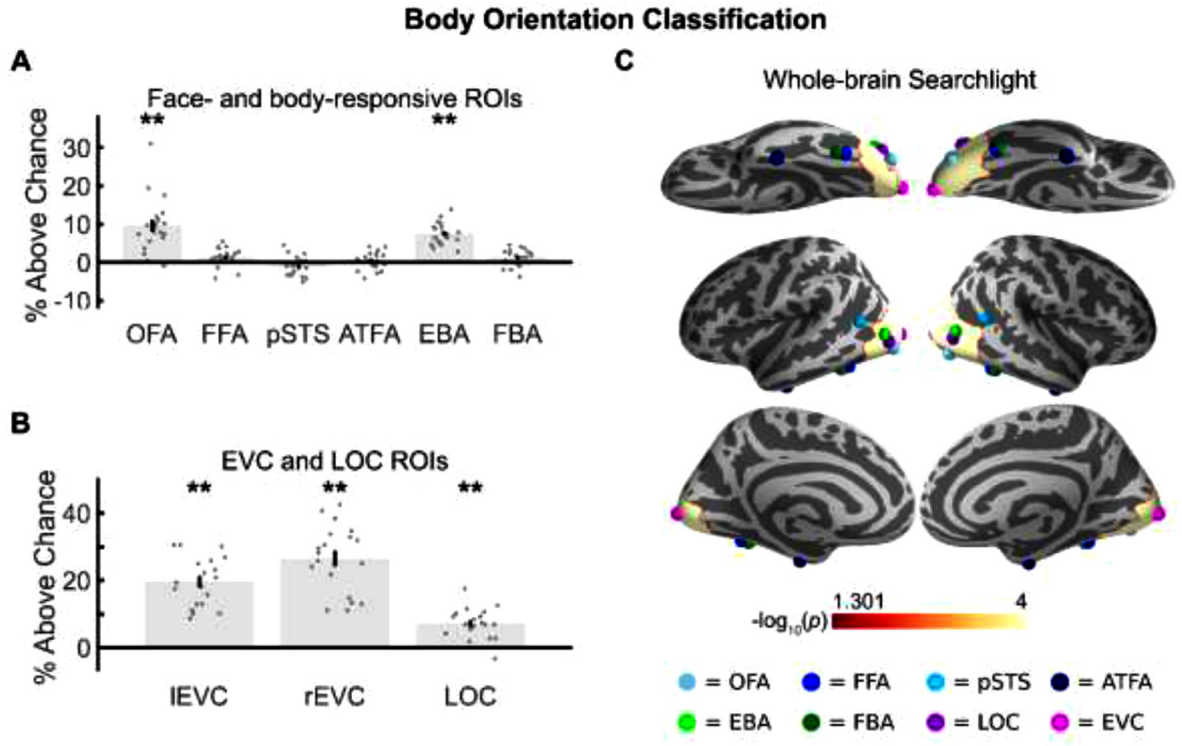

Fig. 7. Classification of body orientation. Classification accuracies for face- and body responsive ROIs (A) and EVC and LOC ROIs (B) are shown as their % above chance-level (1/3). Grey scatter points show classification accuracies for individual participants, ** indicates $p < .001$, * indicates $p < .05$, permutation test and Bonferroni corrected for $N = 9$ ROIs. (C) shows classification of body orientation in a whole-brain searchlight analysis. The scale bar shows $-\log_{10}(p$ values) between 1.301 ($p = .05$) and 4 ($p = 1 \times 10^{-4}$), FWE corrected.

Table 3
Results of paired *t*-tests comparing differences in body orientation classification performance between face- and body-responsive ROIs.

Paired *t*-test	Mean difference	Standard error	*t* value	*p* value	Cohen's d_z
EBA vs. FBA	6.21%	0.772	8.05	< 0.001	1.85
EBA vs. FFA	5.99%	0.720	8.33	< 0.001	1.91
EBA vs. pSTS	8.38%	0.882	9.51	< 0.001	2.18
EBA vs. ATFA	7.14%	0.771	9.26	< 0.001	2.12
OFA vs. FBA	8.77%	1.507	5.82	< 0.001	1.34
OFA vs. FFA	8.55%	1.607	5.32	< 0.001	1.22
OFA vs. pSTS	10.94%	1.601	6.83	< 0.001	1.57
OFA vs. ATFA	9.70%	1.744	5.56	< 0.001	1.28

icant interactions between face/body orientation decoding and ROI or behavioural task. We found a significant interaction between Face/Body orientation and ROI ($F_{8,144} = 7.18, p < .001, \eta_p^2 = 0.29$), but no triple interaction between the three factors ($F_{8,144} = 1.96, p = .056, \eta_p^2 = 0.10$).

Next, we performed follow-up paired *t*-tests between face and body orientation decoding in each ROI to investigate which regions showed significant differences in face and body decoding performance. We found that classification of face orientation was significantly higher than classification of body orientation in the OFA, FFA, pSTS, left EVC and LOC, and body orientation decoding was significantly higher than face orientation decoding in the right EVC. The EBA, FBA and ATFA showed no differences between classification of face and body orientation. Full results of these paired *t*-tests are shown in Table 4.

Table 4
Results of paired *t*-tests in ROIs comparing face vs. body orientation classification performance.

ROI	Mean difference	Standard error	*t* value	*p* value	Cohen's d_z
OFA	7.96%	1.583	5.03	< 0.001	1.13
FFA	2.94%	0.662	4.44	< 0.001	0.99
pSTS	2.22%	0.753	2.95	.008	0.66
ATFA	0.05%	0.740	0.06	.951	0.01
EBA	1.06%	0.985	1.08	.293	0.24
FBA	1.13%	0.734	1.55	.139	0.35
lEVC	3.44%	1.633	2.10	.050	0.48
rEVC	−3.46%	1.600	−2.16	.044	0.50
LOC	3.52%	1.284	2.74	.013	0.61

3.5.2. Searchlight analyses

To investigate whether any other regions showed differences in face and body orientation decoding or an interaction between face/body orientation decoding and behavioural task, we performed a 2 (Face/body orientation classification) x 2 (Task) whole-brain ANOVA. This ANOVA revealed a significant main effect of face/body orientation classification in the left somatosensory cortex, but no other regions. This finding may be due to a difference in participant's responses during the orientation recognition task for face and body stimuli. However, no regions showed a significant interaction between face/body orientation classification and behavioural task.

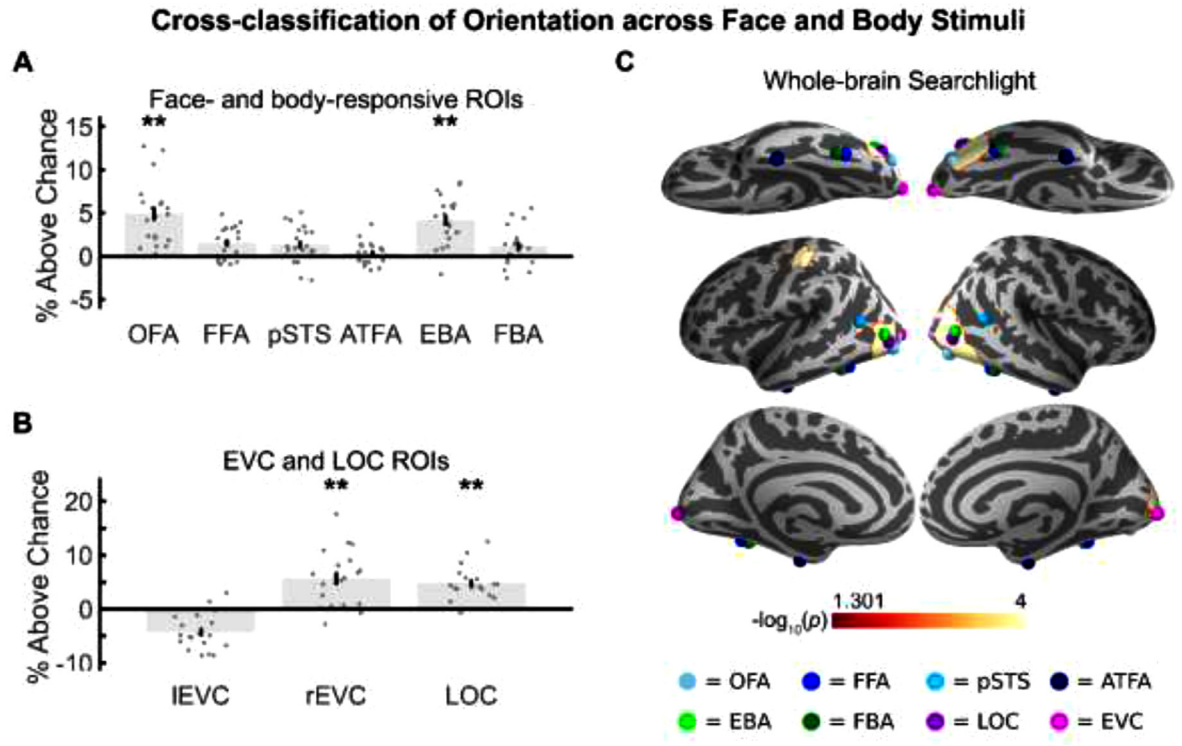

Fig. 8. Cross-classification of orientation across neural activity evoked by face and body stimuli. Classification accuracies for face- and body responsive ROIs (A) and EVC and LOC ROIs (B) are shown as their % above chance-level (1/3). Grey scatter points show classification accuracies for individual participants, ** indicates $p < .001$, * indicates $p < .05$, permutation test and Bonferroni corrected for $N = 9$ ROIs. (C) shows cross-classification of orientation across neural activity evoked by face and body stimuli in a whole-brain searchlight analysis. The scale bar shows $-\log_{10}(p$ values) between 1.301 ($p = .05$) and 4 ($p = 1 \times 10^{-4}$), FWE corrected.

3.6. Classification of orientation across face and body stimuli

We performed classification analyses across neural activity evoked by face and body stimuli to investigate whether any regions contain a neural coding of orientation that could generalise across face and body stimuli. Specifically, we first trained a linear SVM classifier to distinguish between patterns of neural activity evoked by faces of different orientations and then tested this trained classifier on its ability to classify the orientation of neural activity evoked by body stimuli (and vice-versa using neural activity evoked by body stimuli for training the classifier and neural activity evoked by face stimuli for testing it). The results are shown in Fig. 8 and classifier confusion matrices are shown in Fig. S9.

3.6.1. ROI analyses

We first performed a 9 (ROI) x 2 (Task) repeated measures ANOVA to investigate if orientation cross-classification differed across ROIs or behavioural task. We found a significant main effect of ROI ($F_{8,144} = 26.05$, $p < .001$, $\eta_p^2 = 0.59$), but no main effect of behavioural task ($F_{1,18} = 0.01$, $p = .915$, $\eta_p^2 = 0.00$) or interaction between ROI and task ($F_{8,144} = 0.35$, $p = .944$, $\eta_p^2 = 0.02$). Thus, as previously we combined results from the two behavioural tasks for further analyses.

Next, we conducted permutation tests to test which ROIs showed higher than chance (1/3) cross-classification of orientation. Classification of orientation across neural activity evoked by face and body stimuli was significantly above chance-level (1/3) in the OFA (38.2%, $p < .001$ Bonferroni corrected, Cohen's $d_z = 1.34$) and the EBA (37.5%, $p < .001$ Bonferroni corrected, Cohen's $d_z = 1.47$), but not in any other face-responsive ROIs (FFA: 34.9%, $p = .008$ uncorrected, Cohen's $d_z = 0.81$; pSTS: 34.7%, $p = .015$ uncorrected, Cohen's $d_z = 0.62$; ATFA: 33.7%, $p = .301$ uncorrected, Cohen's $d_z = 0.27$) or in the FBA (34.4%, $p = .044$ uncorrected, Cohen's $d_z = 0.48$). We were also able to decode orientation across face and body stimuli from the right EVC (39.0%, $p < .001$ Bonferroni corrected, Cohen's $d_z = 1.07$) and object-responsive LOC (38.2%, $p < .001$ Bonferroni corrected, Cohen's $d_z = 1.62$), but not from the left EVC (29.1%, $p = 1.00$ uncorrected, Cohen's $d_z = 1.26$).

To test whether any overlapping face-responsive voxels might have contributed to our decoding results in the EBA, or whether any overlapping body-responsive voxels might have contributed to our decoding results in the OFA, we conducted follow-up classification analyses with EBA and OFA ROIs with these voxels excluded. We were still able to decode orientation from both ROIs (EBA: 37.2%, $p < .001$ Bonferroni corrected, Cohen's $d_z = 1.34$; OFA: 37.3%, $p < .001$ Bonferroni corrected, Cohen's $d_z = 1.06$).

To test whether orientation cross-classification performance was significantly higher in the face-responsive OFA and body-responsive EBA as compared to face- and body-responsive ROIs that did not show higher than chance orientation cross-classification, we conducted paired *t*-tests between these ROIs. These tests confirmed that orientation classification across face and body stimuli was significantly higher in the OFA and EBA as compared to the FFA, pSTS, ATFA and FBA. Full results of these paired *t*-tests are shown in Table 5.

3.6.2. Searchlight analyses

We conducted whole brain searchlight analyses to see if any additional regions contained patterns of orientation responses that could generalise across face and body stimuli. We first performed a paired *t*-test between searchlight maps from the orientation and identity recognition tasks, to test whether any regions showed differences in orientation classification depending on which behavioural task was performed. We did not find any regions in this analysis, thus we combined results from the two behavioural tasks for further analysis.

Our whole-brain searchlight analysis revealed that bilateral regions overlapping with the OFA, EBA and LOC were able to decode orientation across neural activity evoked by face and body stimuli (Fig 8C),

Table 5
Results of paired *t*-tests comparing differences in orientation classification across face and body stimuli between face- and body-responsive ROIs.

Paired *t*-test	Mean difference	Standard error	*t* value	*p* value	Cohen's d_z
OFA vs. FFA	3.67%	0.785	4.67	< 0.001	1.07
OFA vs. pSTS	3.86%	0.816	4.73	< 0.001	1.09
OFA vs. ATFA	4.79%	0.931	5.14	< 0.001	1.18
OFA vs. FBA	4.06%	0.904	4.49	< 0.001	1.03
EBA vs. FFA	2.79%	0.629	4.44	< 0.001	1.02
EBA vs. pSTS	2.98%	0.859	3.47	.003	0.80
EBA vs. ATFA	3.91%	0.702	5.57	< 0.001	1.28
EBA vs. FBA	3.18%	0.750	4.24	< 0.001	0.97

consistent with our ROI analyses. Interestingly, these regions were located at a point where the LOC, EBA and OFA intersect. Supplemental Figure S10 illustrates the clusters for each participant in relation to the mean locations of LOC, EBA and OFA for each participant. Orientation could also be decoded across face and body stimuli in the right early visual cortex.

3.6.3. Classification of orientation across face and body stimuli separated by training and testing direction

To investigate whether there was any asymmetry in our ability to decode orientation across neural activity evoked by face and body stimuli depending on whether we trained on faces and tested on bodies, or vice-versa, we performed classification analyses separated for these two training and testing directions (Fig S11). We were able to decode orientation significantly above chance from both the OFA (orientation task, train on bodies test on faces: 38.9%, $p < .001$ Bonferroni corrected, Cohen's $d_z = 1.33$; orientation task, train on faces, test on bodies: 38.2%, $p < .001$ Bonferroni corrected, Cohen's $d_z = 0.92$; identity task, train on bodies test on faces: 38.5%, $p < .001$ Bonferroni corrected, Cohen's $d_z = 1.01$; identity task, train on faces, test on bodies: 37.3%, $p < .001$ Bonferroni corrected, Cohen's $d_z = 0.76$) and EBA (orientation task, train on bodies test on faces: 36.6%, $p < .001$ Bonferroni corrected, Cohen's $d_z = 0.92$; orientation task, train on faces, test on bodies: 37.8%, $p < .001$ Bonferroni corrected, Cohen's $d_z = 1.10$; identity task, train on bodies test on faces: 37.7%, $p < .001$ Bonferroni corrected, Cohen's $d_z = 1.08$; identity task, train on faces, test on bodies: 37.7%, $p < .001$ Bonferroni corrected, Cohen's $d_z = 1.00$) for both training and testing directions, but not from any other ROIs. Furthermore, we performed paired *t*-tests to investigate if there were any differences in classification accuracy between the two training/testing directions. We did not find any significant differences in classification accuracy between the two training/testing directions for OFA (orientation task: $t_{19} = 0.67$, $p = .51$, Cohen's $d_z = 0.15$; identity task: $t_{19} = 1.09$, $p = .29$, Cohen's $d_z = 0.24$), EBA (orientation task: $t_{19} = 1.37$, $p = .19$, Cohen's $d_z = 0.31$; identity task: $t_{19} = 0.04$, $p = .97$, Cohen's $d_z = 0.01$) or any other face- or body-responsive ROIs.

3.7. No classification of orientation across face and body stimuli with mean signal

As we found some differences in the mean BOLD responses to faces and bodies of different orientations (Fig. 3 and Fig. 4), we performed a control analysis to examine whether our classification results across neural activity evoked by face and body stimuli were driven by the differences in the mean BOLD signal. To this aim, we repeated the same classification analyses but using only the mean BOLD signal in each ROI, or in each searchlight sphere for training and testing the classifier. If the differences in mean BOLD activation were driving the classification results, we would expect the identical classification results in these new analyses. This was not the case. Results showed that we could not decode orientation in any ROIs using the mean BOLD activation (for details see supplementary Fig S12A-B). Furthermore, whole-brain searchlight analysis only revealed a cluster in the right early visual cortex, but not in any other brain region (see supplementary Fig S12C-D). These results suggest that our decoding of person orientation in EBA and OFA was driven by different patterns of neural activity in these brain regions, rather than by the differences in their overall level of activation. In contrast, classification of person orientation in the right early visual cortex may be partially driven by the differences in the mean BOLD signal.

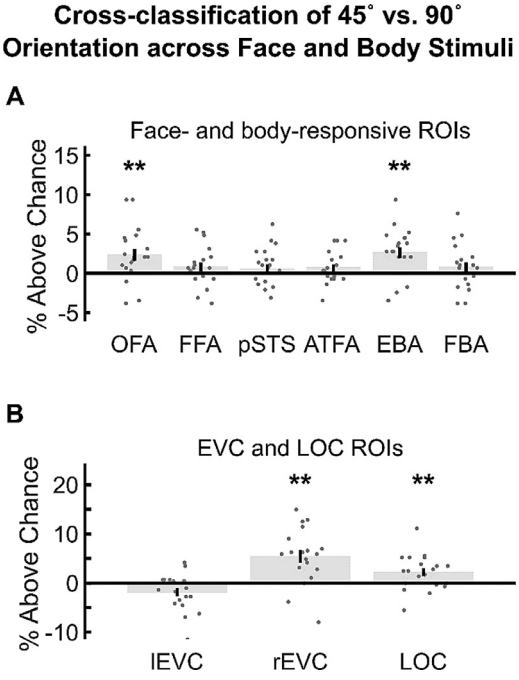

Fig. 9. Cross-classification of 45˚ vs.90˚ orientation across neural activity evoked by face and body stimuli. Classification accuracies for face- and body responsive ROIs (A) and EVC and LOC ROIs (B) are shown as their % above chance-level (1/2). Grey scatter points show classification accuracies for individual participants, ** indicates $p < .001$, * indicates $p < .05$, permutation test and Bonferroni corrected for $N = 9$ ROIs.

3.8. Classification of 45˚ vs. 90˚ orientation across face and body stimuli

As our 0˚ orientation stimuli was symmetric, whereas our 45˚ and 90˚ stimuli were not, it might be possible that our cross-classification results were driven by these differences in symmetry. To address this question, we performed a control analysis to test whether we could decode 45˚ vs. 90˚ orientation across neural activity evoked by face and body stimuli. As both of these stimulus orientations were non-symmetric, successful decoding could not be driven by differences in stimulus symmetry/non-symmetry. Results are shown in Fig. 9.

First, we performed a 9 (ROI) x 2 (Task) repeated measures ANOVA to test whether there were differences in 45˚ vs. 90˚ orientation cross-classification across ROIs or behavioural task. We found a significant main effect of ROI ($F_{8,144} = 7.56$, $p < .001$ Greenhouse-Geisser cor-

Table 6
Results of paired *t*-tests comparing differences in 45° vs. 90° orientation classification across face and body stimuli between face- and body-responsive ROIs.

Paired *t*-test	Mean difference	Standard error	*t* value	*p* value	Cohen's d_z
OFA vs. FFA	1.49%	0.978	1.57	.134	0.35
OFA vs. pSTS	1.82%	1.003	1.86	.078	0.42
OFA vs. ATFA	1.63%	0.900	1.86	.078	0.42
OFA vs. FBA	1.56%	0.995	1.61	.124	0.36
EBA vs. FFA	1.80%	0.900	2.06	.054	0.46
EBA vs. pSTS	2.13%	1.031	2.12	.047	0.48
EBA vs. ATFA	1.94%	0.672	2.97	.008	0.66
EBA vs. FBA	1.88%	0.907	2.12	.047	0.47

rected for non-sphericity, $\eta_p^2 = 0.30$), but no main effect of behavioural task ($F_{1,18} = 0.72$, $p = .408$ Greenhouse-Geisser corrected for non-sphericity, $\eta_p^2 = 0.04$) or interaction between ROI and behavioural task ($F_{8,144} = 2.05$, $p = .081$ Greenhouse-Geisser corrected for non-sphericity, $\eta_p^2 = 0.10$). Therefore, we combined data from the two behavioural tasks for further analyses.

We next conducted permutation tests to determine which ROIs showed higher than chancel-level (1/2) cross-classification of 45° vs 90° orientation. Our results were the same as previously for orientation cross-classification including all three orientations. Cross-classification was significantly above chance-level (1/2) in the OFA (52.3%, $p < .001$ Bonferroni corrected, Cohen's $d_z = 0.68$) and the EBA (52.6%, $p < .001$ Bonferroni corrected, Cohen's $d_z = 0.86$), but not in any other face-responsive ROIs (FFA: 50.8%, $p = .068$ uncorrected, Cohen's $d_z = 0.33$; pSTS: 50.5%, $p = .188$ uncorrected, Cohen's $d_z = 0.16$; ATFA: 50.7%, $p = .112$ uncorrected, Cohen's $d_z = 0.35$) or in the FBA (50.8%, $p = .091$ uncorrected, Cohen's $d_z = 0.27$). As previously, cross-classification was also significantly higher than chancel-level in the right EVC (55.4%, $p < .001$ Bonferroni corrected, Cohen's $d_z = 0.95$) and object-responsive LOC (52.2%, $p < .001$ Bonferroni corrected, Cohen's $d_z = 0.61$), but not in the left EVC (48.1%, $p = 1.00$ uncorrected, Cohen's $d_z = 0.50$).

To test whether any overlapping face- and body-responsive voxels might have driven our decoding results in the OFA and EBA, we conducted follow-up 45° vs. 90° cross-classification analyses in the EBA and OFA ROIs with these voxels excluded. We were still able to decode 45° vs. 90° orientation from both ROIs (EBA: 52.9%, $p < .001$ Bonferroni corrected, Cohen's $d_z = 1.13$; OFA: 52.5%, $p < .001$ Bonferroni corrected, Cohen's $d_z = 0.78$).

To directly test whether 45° vs. 90° orientation cross-classification performance was higher in the OFA and EBA than other ROIs, we conducted paired *t*-tests between these ROIs. These tests showed that 45° vs. 90° orientation cross-classification was significantly higher in the EBA than in the FBA, pSTS and ATFA, but not the FFA. The OFA, however, showed similar cross-classification performance to that observed in the FFA, pSTS, ATFA or FBA. Full results of these paired *t*-tests are shown in Table 6.

3.9. Control analyses for low-level image properties

As our stimuli consisted of natural images of faces and bodies, it is possible that some low-level visual features were more similar across images of the same orientation than across different orientations. This is likely the case for images of face orientations across different identities, and body orientations across different identities, due to similarities in shape. However, it might not be the case for orientations across face and body images, due to the large differences between the visual appearance of faces and bodies. To test the potential influence of low-level visual features on our decoding results, we performed two control analyses.

3.9.1. Pixel intensity correlations

We performed correlations of red, green and blue pixel intensities between images of the same orientation and images varying in orientations, to test whether low-level image information was more similar within the same orientation than across different orientations.

First, we performed the above image-based correlation analysis separately for face and body images, and then we performed a two-sample *t*-test to test whether correlations were significantly higher for images within orientation as compared to across orientation. As expected, same-orientation images showed higher correlations between pixel intensity values than across-orientation images for both face (red: $t_{24} = 7.61$, $p < .001$; green: $t_{24} = 10.72$, $p < .001$; blue: $t_{24} = 11.26$, $p < .001$) and body images (red: $t_{24} = 6.22$, $p < .001$; green: $t_{24} = 6.40$, $p < .001$; blue: $t_{24} = 6.50$, $p < .001$). This result confirms that, within each stimulus category (face or body image), low-level visual information was more similar for within- than across-orientation images.

Second, we performed the image-based correlation analysis across face and body images of the same identity. As previously, we then performed a two-sample *t*-test to test whether correlations were significantly higher for images within orientation as compared to across orientation. We found no significant difference between correlations for red ($t_{16} = -1.22$, $p = .240$), green ($t_{16} = 0.23$, $p = .823$) or blue ($t_{16} = 0.47$, $p = .645$) pixel intensity values, suggesting that low-level image information was not more similar between face and body images of the same orientation as compared to face and body images across different orientations.

3.9.2. Decoding orientation from Gabor-filtered image properties

We also tested whether low-level image properties could support the decoding of orientation across different identities or across face and body images. To do this, we converted our stimulus images into grayscale and then filtered each image using a Gabor-jet model (Lades et al., 1993; Yue et al., 2012). Each Gabor-jet consisted of 80 filters (5 scales x 8 orientations x 2 phases, sine and cosine), and the model consisted of a 10 × 10 uniform grid of nodes placed across each image. The responses from all Gabor-jets for each image thus formed a high-dimensional feature vector containing 8000 features. We then assessed whether we could decode orientation across images when we input these feature vectors into a linear SVM classifier as in our MVPA analyses.

First, we tested whether we could decode orientation across identity from the image feature vectors, separately for face and body stimuli. We trained a classifier to distinguish between feature vectors of 0°, 45° and 90° stimuli from two identities, and then tested the classifier on its ability to decode 0°, 45° and 90° stimuli from the third identity. We performed this separately for feature vectors from the face and body images, and performed each classification analysis three times, with each identity used as the held-out test set once. We then averaged decoding results across the three identities. We found that decoding performance was higher than chance-level (1/3) for both face (55.6%) and body (55.6%) stimuli, suggesting that low-level image information could aid face and body orientation classification across identities.

Second, we tested whether we could decode orientation across face and body stimuli from the image feature vectors. To do this, we trained a classifier to distinguish between feature vectors of 0°, 45° and 90° face

stimuli and then tested the classifier on its ability to decode 0°, 45° and 90° body stimuli, and vice-versa. We then averaged the decoding results across the two training and testing directions. Surprisingly, we found we could decode orientation across face and body image feature vectors (61.1%) at higher than chance-level (1/3), suggesting that low-level image information could allow decoding across face and body stimuli.

Finally, we tested whether the above higher than chance decoding across face and body images was driven by image differences between the symmetric 0° orientation and the non-symmetric 45° and 90° orientations. To test this hypothesis, we performed the same cross-classification analysis across face and body image feature vectors, but included only the 45° and 90° orientation stimuli. In this case, decoding performance was 25%, below the chance-level of 50%. This result suggests that image-based orientation cross-decoding was primarily driven by differences between symmetric and non-symmetric stimuli. In contrast to this, our MVPA results showed consistent cross-decoding of orientation even when only non-symmetric 45° and 90° orientations were included in the classification (see Section 3.8). Together, these results suggest that our cross-decoding results in the occipitotemporal cortex cannot be solely attributed to low-level image properties.

4. Discussion

In this study, we investigated how the brain encodes face and body orientation information by exploring the neural responses to faces and bodies varying in orientation. Our results show that the OFA, EBA, LOC and early visual cortex contain different patterns of neural activity to both faces and bodies of different orientations. More importantly, we found that the OFA, EBA, LOC and right EVC encoded orientation in a stimulus-independent manner. A classifier trained to distinguish patterns of neural activity evoked by face orientations could decode orientation from neural activity evoked by body orientations, and vice-versa. Our study also shows that the FFA responds to face orientation but not to body orientation, suggesting that orientation responses in the FFA are face specific. All these results were consistently observed across two different behavioural tasks, with one requiring attention to the decoded feature (orientation) and the other to identity. These findings highlight both similarities and differences in the neural coding of face and body orientation, demonstrating that face and body orientation information is processed in a partially overlapping brain network.

4.1. Neural coding of face and body orientation in the occipitotemporal cortex

Our results demonstrate that both face and body orientation can be consistently decoded from the neural activity in the face-responsive OFA and body-responsive EBA, as well as the object-responsive LOC and early visual cortex. Previous studies have often separately investigated the neural coding of face and body orientation in face- and body-responsive brain regions respectively, leading to an illusory view that the neural coding of orientation may be stimuli-dependant. For example, several studies have shown that the OFA responds to face orientation (Axelrod and Yovel, 2012; Flack et al., 2019; Guntupalli et al., 2017; Kietzmann et al., 2012), whereas other studies have found that the EBA responds to body orientation (Chan et al., 2004; Ewbank et al., 2011; Taylor et al., 2010; Vangeneugden et al., 2014). Here we show that these regions also encode orientation beyond their preferred stimuli (i.e. the face-responsive OFA also encodes body orientation, and the body-responsive EBA also encodes face orientation), demonstrating that the neural responses to face and body orientation in the OFA and EBA are not face- or body-specific. Furthermore, we also show that the object-responsive LOC encodes both face and body orientation. This finding not only echoes previous research on the neural coding of object and face orientation in the LOC (Axelrod and Yovel, 2012; Ramírez et al., 2014), but also extends this region's orientation sensitivity to body orientation.

The sensitivity of the OFA, EBA, LOC and EVC to both face and body orientation was also found in the mean BOLD response (e.g. Fig. 3 and Fig. 4). In both the EBA and LOC, we found responses progressively increased from 0° to 90° faces and higher responses to 90° bodies compared to 0° and 45° bodies, suggesting a preference for profile views of a person in these regions. Higher neural responses in the LOC to the profile- than front-view faces have also been found in previous studies (Axelrod and Yovel, 2012; Ramírez et al., 2014, faces shown above the fixation condition). In contrast, in the OFA, we found higher responses to 0° and 90° faces compared to 45° faces, and higher responses to 0° bodies compared to 90°bodies. This result is consistent with an earlier study (Axelrod and Yovel, 2012), suggesting a relative preference for front views of a person in the OFA. Similar to the OFA, we also observed a general preference to front view faces and bodies in the EVC, which suggests that the low-level visual features that affect EVC responses to orientation may also influence neural responses in the OFA. Although these results show that the OFA, EBA and LOC respond to both face and body orientation, how these different tuning profiles emerged remains to be elucidated.

Our most remarkable finding was that we could cross-classify orientation across neural responses evoked by faces and bodies in the OFA, EBA, LOC and right EVC, suggesting these regions encode orientation in a stimulus-independent manner. In these brain regions, classifiers trained to distinguish patterns of neural activity evoked by different face orientations could decode patterns of neural activity evoked by body orientations, and vice-versa. Furthermore, our searchlight analyses showed that there was strong classification performance at the intersection of the OFA, EBA and LOC (Fig. 8C), highlighting the contribution of these category-specific brain areas (i.e. face-, body-, and object-responsive) to a shared neural orientation code in the occipitotemporal cortex.

4.2. What processes underlie the shared coding of face and body orientation?

The involvement of the LOC in the coding of orientation leads to the question of whether our results are specific to face and body orientation or whether they would also extend to the coding of general object orientation. Previous work has demonstrated that the LOC is sensitive to object orientation (Andresen et al., 2009; Ewbank et al., 2005; Grill-Spector et al., 1999), and that it contains patterns of activation to both face and object orientations that can generalise across visual field location (Ramírez et al., 2014). Nonetheless, whether faces and objects share the same neural orientation code remains unknown. Furthermore, we note that LOC is traditionally defined by its higher responses to objects compared to scrambled images (Malach et al., 1995), and we found that the LOC showed stronger responses to bodies than to objects, even when voxels overlapping with the EBA were removed (see Section 2.6.). Overlap between the EBA and LOC has also been identified in previous studies (Downing et al., 2007, 2001; Spiridon et al., 2006; Tootell et al., 2015). A recent topographical atlas of category-responsive regions in occipitotemporal cortex also showed face- and body-responsive lateral occipital regions are next to each other without a gap area where the LOC would be expected to be located (Rosenke et al., 2021). Altogether, these results suggest that the LOC may also be involved in body processing, in addition to general object processing. As we did not test objects together with faces and bodies, we were unable to address this question directly in the present study. We speculate that neural coding of face, body and object orientation may be supported by overlapping but dissociable neural mechanisms. Object orientation can be decoded from responses in the EVC and LOC, but not from the FFA (Ramírez et al., 2014), whereas face orientation can be decoded from a broader network including the EVC, LOC, FFA and EBA (Axelrod and Yovel, 2012; Ramírez et al., 2014). Furthermore, some intrinsic differences between face, body and object orientation also suggest that face, body and object orientation may be encoded differently to some extent. Both faces and bodies have an intrinsic orientation that often indicates the focus

of attention of a person, whereas many objects either do not have an intrinsic orientation or do not have an attention-relevant orientation (Foster, 2020; Xu and Franconeri, 2012).

Our cross-classification of orientation in the right EVC suggests that there may be low-level visual features shared by faces and bodies of the same orientation that might contribute to the encoding of orientation. Consistent with this view, we were able to cross-decode orientation based on Gabor-filtered image properties (Section 3.9.2). This decoding seemed to be driven by differences between the symmetric (0°) and non-symmetric orientations (45° and 90°). When we only included the 45° and 90° stimuli for the decoding analysis, image-based decoding failed to classify orientation across faces and bodies. In contrast, we still found robust neural decoding between these two non-symmetric orientations in the OFA, EBA, LOC and right EVC. Moreover, we also tested whether there was low-level RGB colour information that systematically varied across faces and bodies of the same orientation. Our results showed that this was not the case. Together, these results suggest that our orientation cross-decoding in the occipitotemporal cortex cannot be solely attributed to systematic low-level visual properties.

What mechanisms might drive the shared coding of face and body orientation? One possibility is that participants imagined a whole person when viewing face and body stimuli alone. Cox et al. (2004) found that providing a body context with a covered face activated the FFA similarly to viewing an isolated face. Furthermore, imagery of faces and objects has been shown to induce similar neural representations as visual perception of faces and objects, thereby enabling cross-decoding between imagined and perceived categories (Cichy et al., 2012; Reddy et al., 2010).

Another possibility is that both face and body orientation provide an efficient cue for social attention and interaction (Nummenmaa and Calder, 2009; Vestner et al., 2020). Our cross-classification results might be due to a shared neural representation of these attentional cues (e.g. facing towards vs facing away). Consistent with this idea, the EBA shows different neural responses to interacting people than to non-interacting people (Abassi and Papeo, 2020; Walbrin and Koldewyn, 2019). Social orienting based on following the perceived direction of gaze, has also been found to involve a brain region in the occipitotemporal cortex close to the EBA (Marquardt et al., 2017). Our results in EVC are also in line with this possibility. The gradually decreased mean signal in the right EVC (Fig. 3B and 4B), which could be used for cross-classification (Section 3.7), might result from feedback signals of attending to the progressively leftwards direction of faces and bodies (see also Axelrod and Yovel, 2012). As we did not instruct participants to fixate during fMRI scanning, exactly how social attention and eye movements may contribute to the shared coding of face and body orientation remains to be elucidated.

4.3. Neural coding of face and body orientation in the fusiform and anterior temporal cortex

In contrast to our findings in the OFA and EBA, we did not observe stimulus-independent coding of orientation in the face- and body-responsive areas in the fusiform and anterior temporal cortex (i.e. FFA, FBA, and ATFA). For face stimuli, we were able to decode face orientation in the FFA, consistent with previous studies (Axelrod and Yovel, 2012; Guntupalli et al., 2017; Kietzmann et al., 2012; Ramírez et al., 2014). Orientation responses in the FFA seem to be face-specific, as the FFA showed no sensitivity to object orientation in a previous study (Ramírez et al., 2014) or to body orientation in the present study. Furthermore, face orientation classification was significantly higher than body orientation classification in the FFA. We could also decode face orientation from the body-responsive FBA, however, this decoding was not possible when face-responsive voxels were removed from the FBA, suggesting that this decoding was driven by overlapping voxels from the FFA (Schwarzlose et al., 2005). Removing body-responsive voxels from the FFA did not affect decoding performance. In contrast to the FFA, we were unable to decode face orientation from the ATFA. Similar face orientation decoding results were also reported in a previous study (Guntupalli et al., 2017), and this result is consistent with research showing this region is involved in encoding face identity in an orientation-invariant manner (Anzellotti et al., 2014; Guntupalli et al., 2017). However, it is possible that decoding may have been weaker from this region due to the small size of this ROI, or that we could only define it bilaterally in 13 of our 20 participants. Although the ATFA did not exhibit separable patterns of neural activity to different face orientations, it did show stronger responses to frontal faces as compared to 45° or 90° faces (in our univariate analysis). Interestingly, this result is consistent with a finding that the most anterior face-responsive patch in the macaque contains a higher proportion of neurons responding to frontal faces than to other face orientations (Dubois et al., 2015; Freiwald and Tsao, 2010).

For body stimuli, some studies have suggested that the FBA is sensitive to body orientation (Ewbank et al., 2011; Taylor et al., 2010). However, using an MVPA approach, we did not find higher-than-chance classification of body orientation in any of our fusiform or anterior temporal ROIs (i.e. FBA, FFA, and ATFA). Moreover, these areas also showed equivalent mean BOLD responses to the three body orientations. These results suggest that the FBA, FFA and ATFA do not contain unique patterns of neural activity to different body orientations. Our finding that body orientation is encoded in the EBA, but not the FBA, is in line with previous research (Vangeneugden et al., 2014), which showed that the EBA, but not the FBA, contains dissociable information about body facing direction. It is worth noting that while our decoding of body orientation was found in the EBA, but not the FBA, we were able to decode body identity across changes in orientation in the FBA, but not the EBA (Foster et al., 2021). This result suggests that our lack of body orientation decoding in the FBA is not simply due to the small size of this ROI. Furthermore, this result is in line with a recent finding in macaque monkeys. Kumar et al. (2019) found that neurons in the middle STS body patch are more sensitive to body orientation and less sensitive to body identity, than neurons in the anterior STS body patch. Together, these results suggest that neural responses to bodies become increasingly orientation-independent along posterior-anterior hierarchical processing in the occipitotemporal cortex (see Anzellotti et al., 2014; Axelrod and Yovel, 2012; Freiwald and Tsao, 2010 for a similar argument for the neural processing of face orientation).

4.4. Neural responses of the STS to face and body orientation

As to the involvement of the STS in representing face orientation, previous fMRI studies have found mixed results (see Ramírez, 2018, for a review). While some studies have suggested that the STS may encode the orientation of faces (Axelrod and Yovel, 2012; Flack et al., 2019), others found no evidence for face-orientation encoding in the STS (Guntupalli et al., 2017; Ramírez et al., 2014). For body orientation, one human study found that the pSTS did not encode information about body orientation, whereas the EBA did (Vangeneugden et al., 2014). In contrast, in the monkey neurons have been found in the STS that respond to body orientation (Kumar et al., 2019), as well as to orientation shown from both face and body stimuli (Wachsmuth et al., 1994).

With an MVPA approach, we did not find evidence for face or body orientation coding in either our pSTS ROI, or any region of the STS in our searchlight analyses. One possibility is that the STS is more sensitive to dynamic faces and bodies (Pitcher et al., 2011; Reinl and Bartels, 2014; Schultz et al., 2013), whereas we used static face and body stimuli in this study. It has been shown that body walking motion, but not body orientation, could be decoded from the pSTS, suggesting that this region is more sensitive to the direction of biological motion than static orientations (Vangeneugden et al., 2014). Future research using dynamic face and body orientation stimuli may help differentiate the role of STS in encoding person orientation and human motion. Moreover, as the STS is known to be involved in gaze processing (Carlin and Calder, 2013;

Haxby et al., 2000), our results suggest that direction of gaze and orientation of face and body might be processed in different brain regions. In line with this conjecture, previous work has shown that the human anterior STS responds to gaze direction in a head orientation invariant manner (Carlin et al., 2011).

4.5. Visual attention and the neural coding of face and body orientation

Most previous studies that have investigated the neural coding of orientation used tasks that directed attention away from orientation (e.g. brightness discrimination in Ramírez et al., 2014, or detection of identity repetition in Axelrod and Yovel, 2012; Guntupalli et al., 2017). This raises question of whether visual attention modulates the neural coding of orientation. To address this question, we had our participants perform two different behavioural tasks during fMRI scanning, one required attention to stimulus orientation, whereas the other required attention to stimulus identity. We found a remarkable consistence between the results observed under these two conditions, suggesting that attending to orientation information does not necessarily enhance the neural coding of face or body orientation.

One possibility for this task-independent coding of orientation is that attending to identity might involve some automatic processing of face orientation (Axelrod and Yovel, 2012; Guntupalli et al., 2017) or body orientation (Taylor et al., 2010), which might reduce or eliminate the effect of our task manipulation. Note that we did find an attention enhancing effect on identity coding: the identity task produced consistently better decoding results for face and body identity than the orientation task (Foster et al., 2021). Therefore, the lack of task-related neural differences in orientation coding is not due to our behavioural task being too easy to evoke differences in neural responses.

Conclusion

Our study reveals a shared neural coding of face and body orientation in the occipitotemporal cortex. A region located at the intersection of the OFA, EBA and LOC contains separable patterns of neural activity evoked by different orientations, which can generalize across neural activity evoked by faces and bodies. This finding suggests that this region encodes face and body orientation in a stimulus-independent manner. Such stimulus-independent coding of orientation might not be specific to faces and bodies and might also generalise to other objects. Furthermore, we also show that the FFA encodes face orientation, but not body orientation, suggesting that processing of face orientation involves more distributed brain regions than processing of body orientation. Finally, our results demonstrate that visual attention to orientation information does not enhance the neural coding of orientation, suggesting that orientation may be processed automatically. Together, these results not only offer new insights into how the brain encodes an important social interaction cue, face and body orientation, but also provide new evidence for a partially overlapping representation of faces and bodies in the human brain.

Author statement

Celia Foster: Conceptualization; Methodology; Software; Investigation; Formal analysis; Writing - Original Draft; Writing - Review & Editing

Mintao Zhao: Conceptualization; Writing - Review & Editing; Supervision

Timo Bolkart: Methodology; Writing - Review & Editing

Michael J. Black: Methodology; Writing - Review & Editing

Andreas Bartels: Conceptualization; Writing - Review & Editing; Supervision

Isabelle Bülthoff: Conceptualization; Writing - Review & Editing; Supervision

Data and code availability statement

Data cannot be shared as participants were informed that their data would be stored confidentially, in accordance with the rules of the local ethics committee. Code is available at: https://osf.io/uwb48/.

Declarations of Competing Interest

None.

Acknowledgments

This research was supported by the Max Planck Society, Germany.

Supplementary materials

Supplementary material associated with this article can be found, in the online version, at doi:10.1016/j.neuroimage.2021.118783.

References

Abassi, E., Papeo, L., 2020. The representation of two-body shapes in the human visual cortex. J. Neurosci. 40, 852–863. doi:10.1523/JNEUROSCI.1378-19.2019.

Amunts, K., Mohlberg, H., Bludau, S., Zilles, K., 2020. Julich-brain: a 3D probabilistic atlas of the human brain's cytoarchitecture. Science 369, 988–992. doi:10.1126/science.abb4588.

Andresen, D.R., Vinberg, J., Grill-Spector, K., 2009. The representation of object viewpoint in human visual cortex. Neuroimage 45, 522–536. doi:10.1016/j.neuroimage.2008.11.009.

Anzellotti, S., Fairhall, S.L., Caramazza, A., 2014. Decoding representations of face identity that are tolerant to rotation. Cereb. Cortex 24, 1988–1995. doi:10.1093/cercor/bht046.

Axelrod, V., Yovel, G., 2012. Hierarchical processing of face viewpoint in human visual cortex. J. Neurosci. 32, 2442–2452. doi:10.1523/JNEUROSCI.4770-11.2012.

Bannert, M.M., Bartels, A., 2017. Invariance of surface color representations across illuminant changes in the human cortex. Neuroimage 158, 356–370. doi:10.1016/j.neuroimage.2017.06.079.

Bannert, M.M., Bartels, A., 2013. Decoding the yellow of a gray banana. Curr. Biol. 23, 2268–2272. doi:10.1016/j.cub.2013.09.016.

Brainard, D.H., 1997. The psychophysics toolbox. Spat. Vis. 10, 433–436. doi:10.1163/156856897X00357.

Brooks, J.L., 2012. Counterbalancing for serial order carryover effects in experimental condition orders. Psychol. Methods 17, 600–614. doi:10.1037/a0029310.

Carlin, J.D., Calder, A.J., 2013. The neural basis of eye gaze processing. Curr. Opin. Neurobiol. 23, 450–455. doi:10.1016/j.conb.2012.11.014.

Carlin, J.D., Calder, A.J., Kriegeskorte, N., Nili, H., Rowe, J.B., 2011. A head view-invariant representation of gaze direction in anterior superior temporal sulcus. Curr. Biol. 21, 1817–1821. doi:10.1016/j.cub.2011.09.025.

Chan, A.W.-Y., Peelen, M.V., Downing, P.E., 2004. The effect of viewpoint on body representation in the extrastriate body area. Neuroreport 15, 2407–2410. doi:10.1097/00001756-200410250-00021.

Cichy, R.M., Heinzle, J., Haynes, .J..-D., 2012. Imagery and perception share cortical representations of content and location. Cereb. Cortex 22, 372–380. doi:10.1093/cercor/bhr106.

Cox, D., Meyers, E., Sinha, P., 2004. Contextually evoked object-specific responses in human visual cortex. Science 304, 115–117. doi:10.1126/science.1093110.

Dobs, K., Schultz, J., Bülthoff, I., Gardner, J.L., 2018. Task-dependent enhancement of facial expression and identity representations in human cortex. Neuroimage 172, 689–702. doi:10.1016/j.neuroimage.2018.02.013.

Downing, P.E., Jiang, Y., Shuman, M., Kanwisher, N., 2001. A cortical area selective for visual processing of the human body. Science 293, 2470–2473. doi:10.1126/science.1063414.

Downing, P.E., Wiggett, A.J., Peelen, M.V., 2007. Functional magnetic resonance imaging investigation of overlapping lateral occipitotemporal activations using multi-voxel pattern analysis. J. Neurosci. 27, 226–233. doi:10.1523/JNEUROSCI.3619-06.2007.

Dubois, J., de Berker, A.O., Tsao, D.Y., 2015. Single-unit recordings in the macaque face patch system reveal limitations of fMRI MVPA. J. Neurosci. 35, 2791–2802. doi:10.1523/JNEUROSCI.4037-14.2015.

Ewbank, M.P., Lawson, R.P., Henson, R.N., Rowe, J.B., Passamonti, L., Calder, A.J., 2011. Changes in "top-down" connectivity underlie repetition suppression in the ventral visual pathway. J. Neurosci. 31, 5635–5642. doi:10.1523/JNEUROSCI.5013-10.2011.

Ewbank, M.P., Schluppeck, D., Andrews, T.J., 2005. fMR-adaptation reveals a distributed representation of inanimate objects and places in human visual cortex. Neuroimage 28, 268–279. doi:10.1016/j.neuroimage.2005.06.036.

Flack, T.R., Harris, R.J., Young, A.W., Andrews, T.J., 2019. Symmetrical viewpoint representations in face-selective regions convey an advantage in the perception and recognition of faces. J. Neurosci. 39, 3741–3751. doi:10.1523/jneurosci.1977-18.2019.

Foster, C., 2020. The Neural Coding of Properties Shared by Faces, Bodies and Objects. Eberhard-Karls-Universität Tübingen, Germany.

Foster, C., Zhao, M., Bolkart, T., Black, M.J., Bartels, A., Bülthoff, I., 2021. Separated and overlapping neural coding of face and body identity. Hum. Brain Mapp. 1–19. doi:10.1002/hbm.25544.

Foster, C., Zhao, M., Romero, J., Black, M.J., Mohler, B.J., Bartels, A., Bülthoff, I., 2019. Decoding subcategories of human bodies from both body- and face-responsive cortical regions. Neuroimage 202, 1–13. doi:10.1016/j.neuroimage.2019.116085.

Freiwald, W.A., Tsao, D.Y., 2010. Functional compartmentalization and viewpoint generalization within the macaque face-processing system. Science 330, 845–851. doi:10.1126/science.1194908.

Ghuman, A.S., McDaniel, J.R., Martin, A., 2010. Face adaptation without a face. Curr. Biol. 20, 32–36. doi:10.1016/j.cub.2009.10.077.

Gibson, J.J., Pick, A.D., 1963. Perception of another person's looking behavior. Am. J. Psychol. 76, 386–394.

Grill-Spector, K., Kushnir, T., Edelman, S., Avidan, G., Itzchak, Y., Malach, R., 1999. Differential processing of objects under various viewing conditions in the human lateral occipital complex. Neuron 24, 187–203. doi:10.1016/S0896-6273(00)80832-6.

Guntupalli, J.S., Wheeler, K.G., Gobbini, M.I., 2017. Disentangling the representation of identity from head view along the human face processing pathway. Cereb. Cortex 27, 46–53. doi:10.1093/cercor/bhw344.

Haxby, J.V., Hoffman, E.A., Gobbini, M.I., 2000. The distributed human neural system for face perception. Trends Cogn. Sci. 4, 223–233. doi:10.1016/S1364-6613(00)01482-0.

Hebart, M.N., Görgen, K., Haynes, .J..-D., 2015. The decoding toolbox (TDT): a versatile software package for multivariate analyses of functional imaging data. Front. Neuroinform. 8, 1–18. doi:10.3389/fninf.2014.00088.

Kietzmann, T.C., Swisher, J.D., König, P., Tong, F., 2012. Prevalence of selectivity for mirror-symmetric views of faces in the ventral and dorsal visual pathways. J. Neurosci. 32, 11763–11772. doi:10.1523/jneurosci.0126-12.2012.

Kleiner, M., Brainard, D., Pelli, D., 2007. What's new in psychtoolbox-3? Perception 36 ECVP Abstract Supplement.

Kumar, S., Popivanov, I.D., Vogels, R., 2019. Transformation of visual representations across ventral stream body-selective patches. Cereb. Cortex 29, 215–229. doi:10.1093/cercor/bhx320.

Lades, M., Vorbrüggen, J.C., Buhmann, J., Lange, J., von der Malsburg, C., Würtz, R.P., Konen, W., 1993. Distortion invariant object recognition in the dynamic link architecture. IEEE Trans. Comput. 42, 300–311. doi:10.1109/12.210173.

Li, T., Bolkart, T., Black, M.J., Li, H., Romero, J., 2017. Learning a model of facial shape and expression from 4D scans. ACM Trans. Graph. 36, 1–17. doi:10.1145/3130800.3130813.

Loper, M., Mahmood, N., Romero, J., Pons-Moll, G., Black, M.J., 2015. SMPL : a skinned multi-person linear model. ACM Trans. Graph. (Proc. SIGGRAPH Asia) 34 (248), 1-248:16. doi:10.1145/2816795.2818013.

Malach, R., Reppas, J.B., Benson, R.R., Kwong, K.K., Jiang, H., Kennedy, W.A., Ledden, P.J., Brady, T.J., Rosen, B.R., Tootell, R.B.H., 1995. Object-related activity revealed by functional magnetic resonance imaging in human occipital cortex. Proc. Natl. Acad. Sci. U. S. A. 92, 8135–8139. doi:10.1073/pnas.92.18.8135.

Marquardt, K., Ramezanpour, H., Dicke, P.W., Thier, P., 2017. Following eye gaze activates a patch in the posterior temporal cortex that is not part of the human "face patch" system. eNeuro 4, 1–10. doi:10.1523/eneuro.0317-16.2017.

Moors, P., Germeys, F., Pomianowska, I., Verfaillie, K., 2015. Perceiving where another person is looking: the integration of head and body information in estimating another person's gaze. Front. Psychol. 6, 1–12. doi:10.3389/fpsyg.2015.00909.

Natu, V.S., Jiang, F., Narvekar, A., Keshvari, S., Blanz, V., O'Toole, A.J., 2010. Dissociable neural patterns of facial identity across changes in viewpoint. J. Cogn. Neurosci. 22, 1570–1582. doi:10.1162/jocn.2009.21312.

Nichols, T.E., Holmes, A.P., 2001. Nonparametric permutation tests for functional neuroimaging: a primer with examples. Hum. Brain Mapp. 15, 1–25. doi:10.1002/hbm.1058.

Nummenmaa, L., Calder, A.J., 2009. Neural mechanisms of social attention. Trends Cogn. Sci. 13, 135–143. doi:10.1016/j.tics.2008.12.006.

Peelen, M.V., Downing, P.E., 2007. The neural basis of visual body perception. Nat. Rev. Neurosci. 8, 636–648. doi:10.1038/nrn2195.

Perrett, D.I., Smith, P.A.J., Potter, D.D., Mistlin, A.J., Head, A.S., Milner, A.D., Jeeves, M.A., 1985. Visual cells in the temporal cortex sensitive to face view and gaze direction. Proc. R. Soc. London. Ser. B, Biol. Sci. 223, 293–317.

Pitcher, D., Dilks, D.D., Saxe, R.R., Triantafyllou, C., Kanwisher, N., 2011. Differential selectivity for dynamic versus static information in face-selective cortical regions. Neuroimage 56, 2356–2363. doi:10.1016/j.neuroimage.2011.03.067.

Premereur, E., Taubert, J., Janssen, P., Vogels, R., Vanduffel, W., 2016. Effective connectivity reveals largely independent parallel networks of face and body patches. Curr. Biol. 26, 3269–3279. doi:10.1016/j.cub.2016.09.059.

Ramírez, F.M., 2018. Orientation encoding and viewpoint invariance in face recognition: inferring neural properties from large-scale signals. Neurosci. 24, 582–608. doi:10.1177/1073858418769554.

Ramírez, F.M., Cichy, R.M., Allefeld, C., Haynes, .J..-D., 2014. The neural code for face orientation in the human fusiform face area. J. Neurosci. 34, 12155–12167. doi:10.1523/JNEUROSCI.3156-13.2014.

Reddy, L., Tsuchiya, N., Serre, T., 2010. Reading the mind's eye: decoding category information during mental imagery. Neuroimage 50, 818–825. doi:10.1016/j.neuroimage.2009.11.084.

Reinl, M., Bartels, A., 2014. Face processing regions are sensitive to distinct aspects of temporal sequence in facial dynamics. Neuroimage 102, 407–415. doi:10.1016/j.neuroimage.2014.08.011.

Rosenke, M., Van Hoof, R., Van Den Hurk, J., Grill-Spector, K., Goebel, R., 2021. A probabilistic functional atlas of human occipito-temporal visual cortex. Cereb. Cortex 31, 603–619. doi:10.1093/cercor/bhaa246.

Schreiber, K., Krekelberg, B., 2013. The statistical analysis of multi-voxel patterns in functional imaging. PLoS ONE 8, e69328. doi:10.1371/journal.pone.0069328.

Schultz, J., Brockhaus, M., Bülthoff, H.H., Pilz, K.S., 2013. What the human brain likes about facial motion. Cereb. Cortex 23, 1167–1178. doi:10.1093/cercor/bhs106.

Schwarzlose, R.F., Baker, C.I., Kanwisher, N., 2005. Separate face and body selectivity on the fusiform gyrus. J. Neurosci. 25, 11055–11059. doi:10.1523/JNEUROSCI.2621-05.2005.

Spiridon, M., Fischl, B., Kanwisher, N., 2006. Location and spatial profile of category-specific regions in human extrastriate cortex. Hum. Brain Mapp. 27, 77–89. doi:10.1002/hbm.20169.

Taylor, J.C., Wiggett, A.J., Downing, P.E., 2010. fMRI-adaptation studies of viewpoint tuning in the extrastriate and fusiform body areas. J. Neurophysiol. 103, 1467–1477. doi:10.1152/jn.00637.2009.

Tootell, R.B., Echavarria, C., Nasr, S., 2015. A problem of overlap. Vis. Neurosci. 32, E001. doi:10.1017/S0952523814000340.

Vangeneugden, J., Peelen, M.V., Tadin, D., Battelli, L., 2014. Distinct neural mechanisms for body form and body motion discriminations. J. Neurosci. 34, 574–585. doi:10.1523/JNEUROSCI.4032-13.2014.

Vestner, T., Gray, K.L.H., Cook, R., 2020. Why are social interactions found quickly in visual search tasks? Cognition 200, 104270. doi:10.1016/j.cognition.2020.104270.

Wachsmuth, E., Oram, M.W., Perrett, D.I., 1994. Recognition of objects and their component parts: responses of single units in the temporal cortex of the macaque. Cereb. Cortex 4, 509–522. doi:10.1093/cercor/4.5.509.

Walbrin, J., Koldewyn, K., 2019. Dyadic interaction processing in the posterior temporal cortex. Neuroimage 198, 296–302. doi:10.1016/j.neuroimage.2019.05.027.

Wollaston, W.H., 1824. On the apparent direction of eyes in a portrait. Philos. Trans. R. Soc. London 114, 247–256.

Xu, Y., Franconeri, S.L., 2012. The head of the table: marking the "front" of an object is tightly linked with selection. J. Neurosci. 32, 1408–1412. doi:10.1523/JNEUROSCI.4185-11.2012.

Yue, X., Biederman, I., Mangini, M.C., von der Malsburg, C., Amir, O., 2012. Predicting the psychophysical similarity of faces and non-face complex shapes by image-based measures. Vision Res. 55, 41–46. doi:10.1016/j.visres.2011.12.012.